IEEE Access
Multidisciplinary ⋮ Rapid Review ⋮ Open Access Journal

Received 14 March 2023, accepted 29 March 2023, date of publication 5 April 2023, date of current version 20 April 2023.

Digital Object Identifier 10.1109/ACCESS.2023.3264845

RESEARCH ARTICLE

A Comparative Study on Prominent Connectivity Features for Emotion Recognition From EEG

MAHFUZA AKTER MARIA[1], M. A. H. AKHAND[1], (Senior Member, IEEE), A. B. M. AOWLAD HOSSAIN[2], (Senior Member, IEEE), MD. ABDUS SAMAD KAMAL[3], (Senior Member, IEEE), AND KOU YAMADA[3], (Member, IEEE)

[1]Department of Computer Science and Engineering, Khulna University of Engineering and Technology, Khulna 9203, Bangladesh
[2]Department of Electronics and Communication Engineering, Khulna University of Engineering and Technology, Khulna 9203, Bangladesh
[3]Graduate School of Science and Technology, Gunma University, Kiryu 376-8515, Japan

Corresponding author: M. A. H. Akhand (akhand@cse.kuet.ac.bd)

This work was supported in part by the Japan Society for the Promotion of Science (JSPS) Grant-in-Aids for Scientific Research (C) under Grant 21K03930.

ABSTRACT Classifying distinct human emotions, the fundamental purpose of brain-computer interface research, is essential for providing instant personalized services and assistance to individuals. With such emerging applications for individuals, several techniques have been proposed recently to explore interactions between brain regions, such as correlation, synchronization, and dependence. Notably, functional and effective connectivity methods are applied to assess the relationships between different brain areas. The primary objective of this study is to compare the frequently used functional and effective connectivity methods to recognize emotion using Electroencephalogram (EEG) signals. This paper uses a benchmark emotional EEG dataset consisting of 32 channels of EEG signals collected from 32 subjects while they were watching 40 emotional music videos. Specifically, correlation, phase synchronization, and mutual information are used to measure functional brain connectivity, and transfer entropy is used to acquire effective brain connectivity. After extracting the features, they are represented in a two-dimensional connectivity feature map (CFM). The CFMs are then used to classify emotions by a convolutional neural network model. The results of classified emotions are analyzed regarding compatible EEG bands, accuracy, and time. Notably, the Gamma band is found as the most compatible band. The comparative study has demonstrated that though the connectivity method named Pearson correlation coefficient requires less time, the normalized mutual information is the most accurate method with advantageous detecting capability of nonlinear dependencies.

INDEX TERMS Connectivity feature, convolutional neural network, electroencephalography (EEG), emotion recognition, feature extraction.

I. INTRODUCTION

Emotion recognition (ER) is the process of identifying the current mental state of a person, and brain signals are the best tools for recognizing emotions. ER has grown to be an essential part of research in neurology, computer science, medical science and cognitive science [1]. Most commonly, modalities such as facial images [2], speech [3], and gestures [4] can be used to identify emotions. However, these recognition approaches are not ubiquitous and have low recognition accuracy because they depend on the person's age, appearance, culture, language, and habits. Additionally, it is impossible to identify emotions from speech, gesture, or posture for the persons who are physically incapable of speaking or expressing their feelings through gesture or posture, such as the mentally or verbally disabled. According to

The associate editor coordinating the review of this manuscript and approving it for publication was Humaira Nisar.

research in cognitive psychology and neuropsychology, the development and evolution of emotions are strongly related to the functioning of the central nervous system [5]. Therefore, the brain signal is a highly reliable method of recognizing emotions. Brain signal-based ER is being explored in recent studies [5], [6], [7], [8] due to its prospect of being used in different areas like entertainment, virtual worlds, e-learning, instant messaging, online games, and e-healthcare applications [6].

The Electroencephalogram (EEG) has been increasingly popular for researching the brain's reactions to emotional stimuli due to its noninvasiveness, excellent temporal resolution, portable use, and relatively inexpensive and fast [5], [6] in comparison to alternative neuroimaging methods like positron emission tomography [9], functional magnetic resonance imaging [10]. EEG is a technique for capturing the electrical impulses generated by neuronal activities of the brain through its small sensors (i.e., EEG channels) attached to the brain. These signals are anticipated to provide comprehensive information about the emotional process. Delta (0–3 Hz), Theta (4–7 Hz), Alpha (8–12 Hz), Beta (13–29 Hz), and Gamma (30–50 Hz) are the five main types of brain waves that make up the human EEG. These sub-bands may provide more precise information about the constituent neuronal processes' activities [7], [11]. Different mental states and activities are incorporated into the various sub-bands. Emotion has a strong relationship with the Beta and Gamma sub-bands, a weak relationship with the Alpha sub-band, and a very weak relationship with the Theta and Delta sub-bands [8].

There are two standard procedures for emotion classification: the discrete basic emotion description method and the dimension method. Based on the discrete basic emotion description approach, there can be six basic emotion categories, including sadness, joy, surprise, anger, disgust, and fear [12]. According to Russell's model [13], emotions can be characterized using a two-dimensional (2D) space based on levels of Valence and Arousal for the dimension approach. Mehrabian [14] expanded such an emotion model from 2D to 3D, where Dominance is the name of the third dimension. Arousal, which varies from passive (low) to active (high), and Valence, which ranges from negative (unpleasant) to positive (pleasant), dimensions describe how intensely a person feels or the degree of excitement or apathy of emotion. Again, Dominance refers to the ability of a human to exert control over emotion. It can range from submissive (without control) to dominant (empowered) [5], [15], [16]. Due to simplicity and generality, the 2D model of emotion is frequently used in the literature.

Currently, a growing number of researchers are working on ER research. A crucial part of EEG-based ER research is feature extraction. The EEG features extracted from individual channels, such as differential entropy (DE) [17] and power spectral density (PSD) [18], have produced some research results, but these techniques lack functional descriptions of different brain areas. Features extracted from connectivity of multiple channels based on the brain network (i.e., connectivity features) analyze the interaction between brain areas by assessing the dependencies of brain activity, such as causal relationships and correlation. Compared to standard EEG features, these features offer information on the brain's functioning from a different angle [7].

Recently, EEG channel connectivity features mimicking the relationship or connectivity between brain regions, represented in a map called connectivity feature map (CFM), have been widely used in ER. The brain is a vast network of neurons often exhibiting synchronous activities among neurons of various regions, which can provide important information about the neural activity of interest, known as brain connectivity. There are three types of brain connectivity [19]. Anatomical or structural connectivity describes a network of physical connections between groups of neurons or neural components and has to do with the anatomical structure of brain networks [20]. The connectivity can also be based on the functional integration of different brain regions with the directionality consideration. An undirected dependence is known as functional connectivity, and a causal relationship is known as effective connectivity [21]. While functional connectivity assesses the temporal correlation among different active brain regions, effective connectivity assesses how the activity of one brain region influences the other distinct regions [22]. Although all three of these procedures offer valuable information about the brain connectivity behind emotions, the existing studies mainly concentrated on methods of measuring functional and effective connectivity since these have the greatest possibility of revealing the dynamic processes behind emotions. The connectivity of brain regions can be represented as a network where the vertices and lines indicate the cerebral regions and their connections. The weight of the lines represents the connection strength. Then, the adjacency matrix (i.e., CFM) can be formed by taking the strength of connections between brain regions as the elements of the matrix. Several methods can measure the relationship between brain regions, such as Pearson correlation coefficient (PCC) [23], cross-correlation (XCOR), mutual information (MI) [24], partial MI (PMI) [20], phase locking value (PLV) [25], and transfer entropy (TE) [7]. XCOR and its variant PCC are linear functional connectivity, MI and PLV are non-linear functional connectivity, and TE is effective non-linear connectivity. PCC and XCOR can detect linear dependencies, MI measures shared information, PLV represents phase synchronization, and TE measures directed information flow between two brain regions.

This study aims to perform emotion classification from connectivity matrices using deep learning (DL) and analyze the results for different connectivity measures to find the best-suited connectivity method for ER from EEG. Convolutional neural network (CNN), the prominent DL method, is used for emotion classification in the two-dimensional Valence Arousal model as it automatically extracts internal

features. The major contributions of the present comparative study are summarized as follows:

1) A systematic review of ER from EEG signals has been conducted, emphasizing connectivity feature-based methods to narrow down the number of compatible features targeting more close investigation.
2) Six selected connectivity feature maps are constructed from the segmented and filtered raw EEG signals and investigated under a suitable experimental environment (not biased to any individual one) to expose the proficiency of individual methods. The normalized mutual information feature is found most accurate with advantageous detecting capability of nonlinear dependencies which is identified as a new finding as far our knowledge.
3) A customized CNN has been designed to classify emotions using the constructed CFMs. The CNN classifier performance has been evaluated using widely accepted evaluation matrices.
4) Aiming a profound study, rigorous comparative analysis has been conducted among six CFM methods for ER using a benchmark DEAP dataset considering compatible EEG bands, classification accuracy, and computation time to reach impactful conclusions. Achieved ER performance from this study also compared with the related state-of-the-art studies.

The rest of this paper is organized as follows. Section II describes the related articles of this work. Section III presents the overall emotion recognition process, including data preprocessing, feature extraction, and classification. In Section IV, the experimental setup and experimental results are described. Section V contains some discussion on experimental results. At last, Section VI concludes the paper by discussing the limitations of this study and possible future research.

II. LITERATURE REVIEW

EEG has been well-studied to investigate how the brain reacts to emotional experiences. Typically, machine learning (ML) or DL methods are used for ER using extracted features from EEG signals. Several ER studies are available using different feature extraction and classification techniques. The features broadly fall under the categories of individual channel features and connectivity features. The following subsections review prominent ER studies categorically based on the EEG features' type.

A. ER USING INDIVIDUAL CHANNEL FEATURES

Individual channels are considered independent signal sources in the respective channel feature category, and the characteristic(s) of signal from a particular channel are exposed as feature value(s). Generally, features are extracted from EEG signals in the time domain (e.g., fractal dimension (FD), statistical characteristics (SC)), frequency domain (e.g., SC, PSD), and time-frequency domain (e.g., discrete wavelet transform, entropy). Among the features from different domains, entropy features (e.g., sample entropy, approximate entropy, DE, wavelet entropy), FD, Hjorth Parameters (HP), Hurst exponent, Lyapunov exponent, etc., are used to analyze the nonlinear dynamics of the EEG signals. These features are used by some ML or DL models for classification. The representative studies are summarized in Table 1.

Pioneer studies considered different ML methods to classify emotions from different time and frequency domain features [18], [26], [27], [28], [29], [30]. Support vector machine (SVM) was used by Liu et al. [18] to identify cross-stimulus as well as within-stimulus discrete emotional states (e.g., happiness, sadness) from PSD features selected by SVM-recursive feature elimination (RFE) from different frequency bands which identified that the higher frequency band roughly occupied the larger contribution part. The study [18] also showed that, shared non-emotional information in the samples from the same stimuli would make the classifier easier to recognize the testing sample accurately. Mert and Akan [26] used the time-frequency features of EEG signals obtained by the multivariate synchrosqueezing transform (MSST) to classify emotions between the binary states (high vs. low) of Arousal and Valence using a fully connected neural network (FNN). In the study [26], independent component analysis (ICA), and feature selection were applied to reduce the high dimensional 2D time-frequency distribution. Jagodnik et al. [27] investigated correlation, MI and principal component analysis (PCA), sequential backward selection (SBS), sequential forward selection (SFS), sequential forward floating selection (SFFS) for feature selection including SC, HP, DE, band energies, power, Wavelet entropy. They used a multi-classifier fusion method, combining k-nearest neighbors (KNN), SVM, and random forest (RF) for classification; and it found that MI is better than PCA and correlation and combination of SFFS with MI shows better than MI. To reduce the burden of large feature set employment, HP (activity) was extracted in frequency domain by Mehmood et al. [28], where RF was used as a classifier. Hybrid features were extracted by Pane et al. [29] that consist of time, frequency (PSD), and time-frequency (wavelet) domain features. Time domain features include signal average, band power, standard deviation, kurtosis, skewness, maximum peak, and zero-crossing number. The study [29] considered different time, frequency and time-frequency domain features to classify emotion using SVM, linear discriminant analysis (LDA) and RF. The study identified that happy and relaxed are dominant in the left hemisphere, while angry and sad emotions are better recognized from the right hemisphere. Statistical features can be extracted in both time and frequency domains, as in the study [30], where four emotional states were classified based on the least square SVM and naive Bayesian (NB) classifier; the study identified that predicting emotions for different subjects can be incorrect without personalized EEG training data. Subasi et al. [31] used tunable Q wavelet transform in the feature extraction step and rotation forest ensemble (RFE)

TABLE 1. Representative existing ER studies using individual channel feature.

Ref.	Year	Feature			Classifier	Remarks
		Time	Frequency	Time-frequency		
[33]	2017		PSD		RNN + CNN	Shorter time window provides more details information.
[17]	2018		DE		HCNN	HCNN is efficient especially on Beta and Gamma waves.
[18]	2018		PSD		SVM	Shared non-emotional information from the same stimuli produce better within-stimulus ER accuracy.
[26]	2018			MSST	FNN	MSST and ICA are promising methods and combinations.
[35]	2018		DE, PSD		GCNN	Combined feature from multiple frequency bands are better than individual frequency band.
[29]	2019	SC and zero crossing number.	Band power, PSD	Wavelet	SVM, LDA, RF	Happy and relaxed are better recognized from left hemisphere, while angry and sad are from right hemisphere.
[16]	2020	SC			CNN + SAE + DNN	Adding autoencoder can speed up model training.
[30]	2020	SC	SC		SVM + NB	Predicting emotions for different subjects can be incorrect without personalized EEG training data.
[36]	2020	FD	DE, PSD		SRU + EL	The model can solve the problem of long-term dependencies occurrence in normal RNN.
[31]	2021	Tunable Q wavelet transform			RFE	The approach is lightweight and its mathematical models are simple.
[34]	2021	FD, HP, peak-to-peak, root-mean-square	Band power, DE, PSD		CNN + SVM	HOLO-FM method outperforms TOPO-FM
[27]	2022	SC, HP, sample entropy, approximate entropy etc.	DE, band energies, power	Wavelet entropy	KNN + SVM + RF	Applied feature selection, MI is better than PCA and correlation, and MI + SFFS is better than MI.
[28]	2022		HP		RF	HP in frequency domain can reduce the burden of employing a large feature set.
[32]	2022	FD, Teager and instantaneous energy			SVM, NB, KNN, CNN	Shorter segments provide more accuracy.
[37]	2022	SC, HP, FD, Hurst, entropy etc.	PSD, wavelet entropy, etc.		DNN	The overall recognition effect on the Valence dimension is the best, followed by Arousal, and the worst is Liking.

classifier; the approach is lightweight and its mathematical models are simple.

While studies mentioned above used conventional ML models, DL methods were used in recent studies for emotion analysis as such methods extract relevant features through their embedded learning process. Luo et al. [16] extracted SC (variance, mean, kurtosis, and skewness) of the EEG signal as time domain features and used a combined CNN + sparse autoencoder (SAE) + deep neural network (DNN) model to classify emotions and showed that their model requires less epochs to be trained than CNN. DE was employed with Hierarchical CNN (HCNN) by Li et al. [17] to classify three types of emotions (positive, neutral, and negative) and showed that HCNN is efficient in ER especially on Beta and Gamma waves. Moctezuma et al. [32] used Teager and instantaneous energy, Higuchi and Petrosian FD as time domain feature and SVM, NB, KNN, CNN as classifier for ER according to Valence and Arousal scale from EEG channels selected by multi-objective evolutionary algorithm. In the study, three segmentation time windows (2, 5, and 10 s) were tested and the best results obtained from 2s segment. Meanwhile, Li et al. [33] designed a hybrid model incorporating recurrent neural network (RNN) and CNN for emotion classification in the Valence-Arousal plane by using topographies of the PSDs of the EEG signals with different length time windows; it was identified that a short time window provides more details information. In the study [34], a combined CNN + SVM model was used to classify emotions and two feature map creation methods were proposed based on the topographic (TOPO-FM) and holographic (HOLO-FM) representation of different features such as FD, HP, peak-to-peak, root-mean-square, band power, DE, and PSD features where HOLO-FM outperformed TOPO-FM in all cases. DE feature and PSD feature from five frequency bands were also investigated by Song et al. [35] with dynamical graph CNN (GCNN) where higher frequency bands were identified as better than lower frequency bands. ER was performed using a simple recurrent units (SRU) network and ensemble learning (EL) which has the ability to solve the problem of long-term dependencies occurrence in normal RNN by Wei et al. [36], where the mean absolute value, PSD, fractal dimension, and DE features were used for the nonlinear analysis of the EEG signals. Hurst exponent, sample entropy, HP, vector autoregression, wavelet entropy, spectral entropy, and PSD features were extracted by [37], where DNN was employed for ER in three dimensions, i.e., Valence, Arousal, and Dominance. The overall recognition effect on the Valence dimension was the best, followed by Arousal, and the worst was Liking.

B. ER USING CONNECTIVITY FEATURE

EEG connectivity feature is mainly based on connections in brain regions. However, it is widely accepted that a network connects the brain's regions, where the interactions between

the network's nodes may interpret brain activities. Thus, emotion analysis seems beneficial in measuring the relationship between several brain areas, and several existing ER studies have revealed the effectiveness of CFM with connectivity features. The representative ER studies that used connectivity features are summarized in Table 2.

Khosrowabadi et al. extracted magnitude mutual information and squared coherence estimate (MSCE) and MI features, where KNN and SVM classifier from where it was identified that different kinds of functional brain connectivity exist in different emotional states [38]. Petrantonakis and Hadjileontiadis used SVM as classifier and a new feature was introduced namely asymmetry index (AsI) from the multidimensional directed information (also known as partial transfer entropy (PTE)) of relaxed and emotional state [39] where higher AsI values indicate more effective emotion elicitation trials. The feature vector set from the AsI feature was constructed based on two methods, i.e., higher order crossings (HOC) and XCOR, and the results identified that HOC method is superior against XCOR.Gao et al. used Granger causality (GC) and TE features, with three classifiers, SVM, RF, and decision tree (DT) [5]; TE feature was identified as more suitable than GC and SVM classifier was better than RF and DT. TE feature was also used by the study [40] and [41]. PCC, PLV and phase-amplitude synchronization (PAC) was used by Wang [42] where brain network was constructed by taking the cross-frequency coupling (CFC) intensity of Theta and Gamma bands. Naser and Saha [43] used Spearman's rank correlation with SVM to investigate the influence of music liking on the induced emotions; the best results obtained using low liking music videos for Arousal and Dominance scales, whereas high liking data provides the best results for Valence scale. Kılıç and Aydın used SVM classifier with radial basis function (RBF) and Gaussian kernel while PCC and Spearman correlation was used to extract feature; better performance was obtained by RBF with longer segmentation time window [44]. Zanetti et al. used MI, partial MI (PMI)) and entropy features inside one CFM, where the RF was used as classifier for stress assessment [45]; the study suggested that brain-heart interactions are less involved in the differential characterization of mental stress compared to a relaxed state. PCC, PLV, and MI extracted from different sub-bands were used with SVM classifier for the binary classification of emotional states (high vs. low for Valence and Arousal) by Chen et al. [46], where Gamma frequency band identified as more effective for Valence levels identification. PLV feature was also used by the study [47], [48], [49]. Khosrowabadi used three effective connectivity features (i.e., phase slope index (PSI), direct transfer function (DTF), and generalized partial directed coherence (GPDC)) with KNN and SVM classifiers; results identified that PSI is better than DTF and GPDC [50]. Wang et al. used SVM classifier where normalized MI (NMI) was used as feature; the CFMs identified that wider range of activated brain regions exist in high Arousal low Valence (HALV) state [51]. SVM was also used in the study [52], [53], [54], [55] with PLV, local activation features,PLV, DE, common spatial pattern features, phase lag index (PLI), PVL, DE, PSD features, MI, spectral power features respectively; outcomes of these study showed that combined feature provide better results than individual feature. The study [55] also identified RBF as better than sigmoid kernel.

Several existing studies considered CNN and other DL methods for ER from CFMs. Among different emotional dimension (e.g., Valence, Arousal, Dominance, Liking, and Familiarity), Kumagai et al. classified Familiarity with SVM and DNN where XCOR was used as feature; results identified that SVM is better than DNN to recognize Familiarity [56]. Moon et al. used PCC, PLV and PLI features, where SVM and CNN were used as classifiers [21]. The author of the study [21] showed that CNN could improve classification performance in comparison to SVM and the electrode ordering in CFM has great effect in ER. Different ordering of electrodes was investigated in the study [7] for emotional EEG classification with PCC, PLV and TE; data-driven channel ordering was exposed to be better than random ordering. Feature fusion approach was used by Guo et al. with connectivity feature PCC and synchronization likelihood (SL) where ensemble of CNN was used for classification and higher ER accuracy obtained in Valence dimension than Arousal dimension [57]. Wang et al. used PSI with CNN and showed that connectivity feature shows superior performance, compared with the input of raw EEG data [58]. Graph neural network (GNN) was employed by Liu et al. where weighted PLI (wPLI) was used as feature [59]. The study [59] suggest that emotional processes may not limit to single-frequency band communication but rely on multi-frequency associations. Bao et al. proposed a model combining multi-layer dynamical graph convolution network (MDGCN)with style-based recalibration CNN (SRCNN)for classification with PCC; the proposed model combined shallow layer and deep layer features that improved the recognition performance [60]. Wang et al. used a PDC with graph CNN where recognition accuracy was higher in Valence dimension than Arousal dimension [61]. Zheng et al. [62] used linear graph CNN with connectivity features PCC, PLV and TE where recognition accuracy was higher in Arousal dimension than Valence dimension. Islam et al. [8] and Jin and Kim [63] also used PCC feature, where CNN and long short-term memory (LSTM) + multi-layer perceptron (MLP) were used for ER, respectively. The CFMs from different persons presented in the study [63] revealed that different connectivity patterns exist in different persons even they are in the same emotion. PDC and direct DTF (dDTF), were used in two studies [64] and [65] by Bagherzadeh et al., where several pre-trained CNN models were used as classifier. The best results attained from Alpha frequency band with ResNet-18 and ResNet-50 in the study [64] and [65], respectively. Chao et al. [66] used maximal information coefficient (MIC) for feature extraction, PCA network (PCANet) based DL model was also used

TABLE 2. Representative existing ER studies using connectivity feature.

Ref.	Year	Connectivity Method		CFM Dimension	Classifier	Remarks
		Functional	Effective			
[38]	2010	MSCE, MI		-	SVM, KNN	Functional brain connectivity varies with emotional states.
[39]	2011	XCOR	PTE	1D	SVM	HOC method is superior against XCOR.
[46]	2015	PCC, PLV, MI		2D	SVM	Gamma band is more effective for Valence classification.
[55]	2017	MI		-	NB, SVM	RBF kernel is preferable to sigmoid kernel.
[56]	2017	XCOR		-	SVM, DNN	SVM is better than DNN to recognize Familiarity.
[21]	2018	PCC, PLI, PLV		3D	SVM, CNN	Channel ordering in CFM is important for ER.
[50]	2018		PSI, DTF, GPDC	1D	KNN, SVM	PSI is more suitable than DTF and GPDC.
[45]	2019	MI, PMI		2D	RF	Brain-heart interactions are highly related to the differential characterization of relaxed state than mental stress.
[51]	2019	NMI		2D	SVM	More brain regions are activated in HALV state.
[57]	2019	PCC, SL		2D	CNN + EL	Higher accuracy obtained in Valence than Arousal dimension.
[5]	2020		GC, TE	1D	SVM, RF, DT	TE is better than GC. SVM is better than RF and DT.
[7]	2020	PCC, PLV	TE	3D	CNN	Data-driven channel ordering is better than random ordering.
[16]	2020	PCC		3D	CNN + SAE + DNN	Adding autoencoder can speed up model training.
[63]	2020	PCC		2D	LSTM + MLP	Connectivity features varied from person to person.
[66]	2020	MIC		2D	PCANet + SVM, CNN	PCANet + SVM performs better than CNN.
[8]	2021	PCC		2D	CNN	Proposed CFM can reduce time and memory requirement.
[42]	2021	PCC, PLV, PAC		2D	SVM	Constructed brain network based on Theta-Gamma CFC.
[43]	2021	Spearman's rank correlation		-	SVM	Investigated the influence of music liking on the induced emotions.
[58]	2021		PSI	-	CNN	Connectivity feature provides higher accuracy than raw data.
[23]	2022	PCC, COH, PLV	TE	2D	DARCNN	PLV is better than PCC, COH and TE.
[44]	2022	PCC, Spearman correlation		-	SVM	RBF is better than Gaussian kernel. Higher accuracy obtained with longer segmentation.
[54]	2022	PLV, PLI		-	SVM	Combined features give better results than individual features.
[59]	2022	wPLI,		-	GCNN	Emotional processes rely on multi-frequency associations.
[60]	2022	PCC		-	MDGCN + SRCNN	Combination of shallow layer and deep layer features can improve the recognition performance.
[61]	2022		PDC	-	GCNN	Higher accuracy obtained in Valence than Arousal dimension.
[62]	2022	PCC, PLV	TE	2D	Linear GCNN	Higher accuracy obtained in Arousal than Valence dimension.
[64]	2022		PDC	2D	Pretrained CNN	Alpha band is suitable with ResNet-18.
[65]	2022		dDTF	2D	Pretrained CNN	Alpha band is suitable with ResNet-50.
[67]	2022	PCC, NMI		-	Compact convolution network + auxiliary fully connected network	Can effectively reconstruct high-density EEG and holds potentials in EEG big data applications.
[68]	2023	PCC		-	Convolutional graph attention network	Positive emotion shows stronger functional connectivity than negative emotions.

for deep feature extraction from MIC feature; both features were classified with SVM, the deep feature also classified with CNN; the higher accuracy achieved with PCANet + SVM model. Liu et al. used PCC with CNN + SAE + DNN model and showed that the proposed model take less epoch to be trained than the traditional CNN model [16]. Chen et al. used three functional connectivity (i.e., PCC, COH and PLV), an effective connectivity (i.e., TE) features, and domain adaptive residual CNN (DARCNN) was used as classifier; the best result was achieved with PLV feature [23]. The studies of [16], [21], and [23] revealed that connectivity features improve the performance over individual channel features. Tang et al. used PCC and NMI to extract feature and investigated a DL model (combining a compact convolutional network and an auxiliary fully connected network) which can effectively reconstruct high-density EEG and holds potentials in EEG big data applications [67]. Convolutional graph attention network was used by Li et al. [68], where PCC was used as feature. The study [68] indicates that functional connection strength under high Valence is higher than that under low Valence, i.e., the positive emotion shows stronger functional connectivity than negative emotions.

C. OBSERVATIONS FROM THE EXISTING STUDIES: STUDY MOTIVATION

Different features extracted from individual channel, as well as connectivity of multiple channels, have been used for ER by a significant number of researchers recently. In the first approach, various time domain or frequency domain features were extracted from each channel and fed to the ML or DL models to classify them. Among the individual features, PSD [37], DE [17], HP [34], [37], etc., were frequently used feature. Recently, EEG channel connectivity features have been widely used in ER, and several studies have demonstrated the effectiveness of connectivity features for ER. Among the functional connectivity, PCC, PLV, and MI were used frequently in the literature, such as PCC

was used by the study [7], [8], [21], [23], [42], [44], [46], [60], [62], [63], [67], [68], PLV was used by the study [7], [21], [23], [25], [42], [47], [48], [49], [52], [53], [54], [62] and MI was used by the study [24], [38], [45], [46], [55]. The EEG connectivity features for classification are typically extracted at the functional brain network level. A few studies used effective connectivity for ER. Among the effective connectivity, TE is the mostly used method, which was used in the study [5], [7], [23], [40], [41], [62]. Besides, there are several connectivity methods, such as PLI [21], PSI [50], PDC [64], and GC [5]. Among the various classification algorithms, CNN-based classifiers are the most popular. Several other prominent classifiers are SVM, KNN, RF, NB, and hybrid models. It might be interesting to investigate the performance of the popular connectivity methods and their variants in the same framework. This study has investigated several popularly used connectivity strategies in ER investigations, reflecting diverse aspects of brain connectivity. The connectivity method from where these popular connectivity methods are originated and their variants are also investigated, which are described in Table 3. Different studies investigated these prominent connectivity features with different settings, and it is timely demand to investigate those in a common framework to identify individuals' proficiency, which is the primary motivation of this study.

III. EMOTION RECOGNITION FROM EEG USING CONNECTIVITY FEATURE MAP AND CNN

ER from EEG signals can be summed up in three steps: pre-processing the signals, feature extraction, and identifying emotions using these features. Fig. 1 demonstrates the ER system, where XCOR, PCC, PLV, MI, NMI, and TE connectivity methods are considered for extracting features. Then CNN is used for ER using the features. The following subsections describe the major steps of the ER system.

A. BENCHMARK DATASET

In this study, the Database for Emotion Analysis using Physiological Signals (DEAP) [69] is used for emotion analysis. DEAP is one of the largest EEG database for emotion analysis. It contains EEG and peripheral physiological signals from 32 subjects (i.e., individuals) captured while they were watching 40 emotional music videos. In addition, subjective scores that quantify the levels of Valence, Arousal, Liking, and Dominance of the emotional states range between 1 to 9 (only linking ranges from 1 to 5) induced by watching the videos are included in the database. Emotions can be majorly categorized using a 2D space based on levels of Valence and Arousal considering the dimension approach. Valence ranges from unpleasant (negative) to pleasant (positive), and Arousal ranges from passive (low) to active (high), which indicate how strongly human feels emotions. The DEAP database uses the BioSemi ActiveTwo system to record data. The EEG electrodes are placed according to the 10/20 international standard. At the time of EEG data acquisition, the electrode has to be connected to the scalp. The name of the electrodes originates from the names of the brain lobes [70] where the electrode is to be placed. F stands for Frontal lobe, T for Temporal lobe, C for Central region, P for Parietal lobe, and O for Occipital lobe. The z (zero) refers to an electrode position at the midline. Likewise, PO corresponds to the electrode at the Parietal-Occipital lobe. The standard 10/20 system sets of electrodes locations on the skull is shown in Fig. 2.

The pre-processed EEG signals provided in the database are used in this study that had undergone downsampling to 128 Hz, EOG artifacts were removed, a bandpass frequency filter from 4.0-45.0Hz was applied and the data was segmented into 60 second trials and a 3 second pre-trial baseline removed. The downloaded pre-processed version of the DEAP dataset contains 32 files for 32 participants. Each participant file contains two arrays named data and labels as shown in Table 4. The videos are in the order of experiment id, so not in the order of presentation. This means the first video is the same for each participant. There are 40 channels, where the first 32 channels are for EEG signals, and the rest are peripheral physiological signals. In the pre-processed version of the dataset, the EEG channels are ordered as listed in Table 5.

B. PRE-PROCESSING

Pre-processing is a common step in working with EEG signals, which includes filtering the signals, removing artifacts, etc. The EOG artifacts are removed in the pre-processed version of the DEAP dataset. Reshaping, filtering, and segmentation are applied to the signals as the further pre-processing steps.

1) RESHAPING

In the dataset, the signal length is 63 seconds: the first 3 seconds of data is the pre-trial baseline, which is removed as it doesn't contain any information relating to emotion, and the last 60 seconds of data is processed for this study. With the sampling frequency 128Hz, the number of data points stands at $60 \times 128 = 7680$. Among 40 channels, EEG data is contained in 32 channels, which are chosen for this experiment. After reshaping, the data format is changed from video/trial $\times$ channel $\times$ data $= 40 \times 40 \times 8064$ to video/trial $\times$ channel $\times$ data $= 40 \times 32 \times 7680$.

2) FILTERING

It is reported in literature that emotion has a strong relation with the Beta and Gamma sub-bands and a weak relation with the Alpha sub-band whereas a very low relation with the Theta and Delta sub-bands of EEG [8]. Therefore only the Alpha, Beta and Gamma sub-bands are considered in this study and the filtering is performed to extract these bands from EEG signal with an open-source toolbox EEGLAB [71]. Sample of original EEG signal and its Alpha, Beta, and Gamma sub-band signals are shown in Fig. 3.

TABLE 3. Prominent connectivity features and their usages statistics.

Connectivity Type	Connectivity Method	First Used in EEG-Based ER Study		Remarkable ER Studies with the Feature
		Ref.	Year	
Functional linear (Classical measures)	XCOR	[39]	2011	[39], [56]
	PCC	[46]	2015	[7], [8], [21], [23], [42], [44], [46], [60], [62], [63], [67], [68]
Functional non-linear (Phase-based measures)	PLV	[46]	2015	[7], [21], [23], [25], [42], [47]–[49], [52]–[54], [62]
Functional non-linear (Information theoretic measures)	MI	[38]	2010	[24], [38], [45], [46], [55]
	NMI	[51]	2019	[51], [67]
Effective non-linear (Information theoretic measures)	TE	[7]	2020	[5], [7], [23], [40], [41], [62]

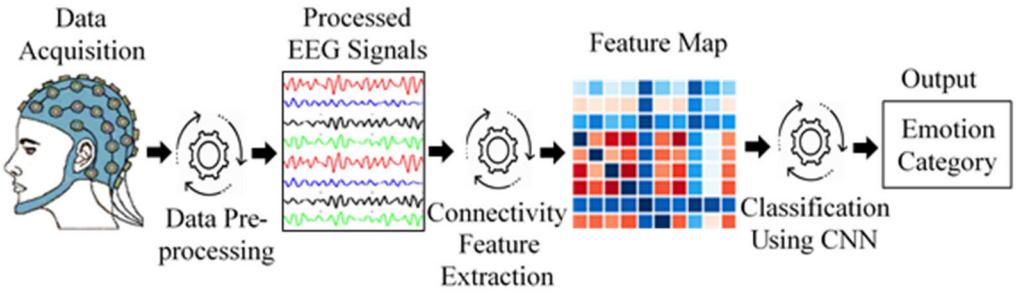

FIGURE 1. Framework of the ER system from EEG using CFM.

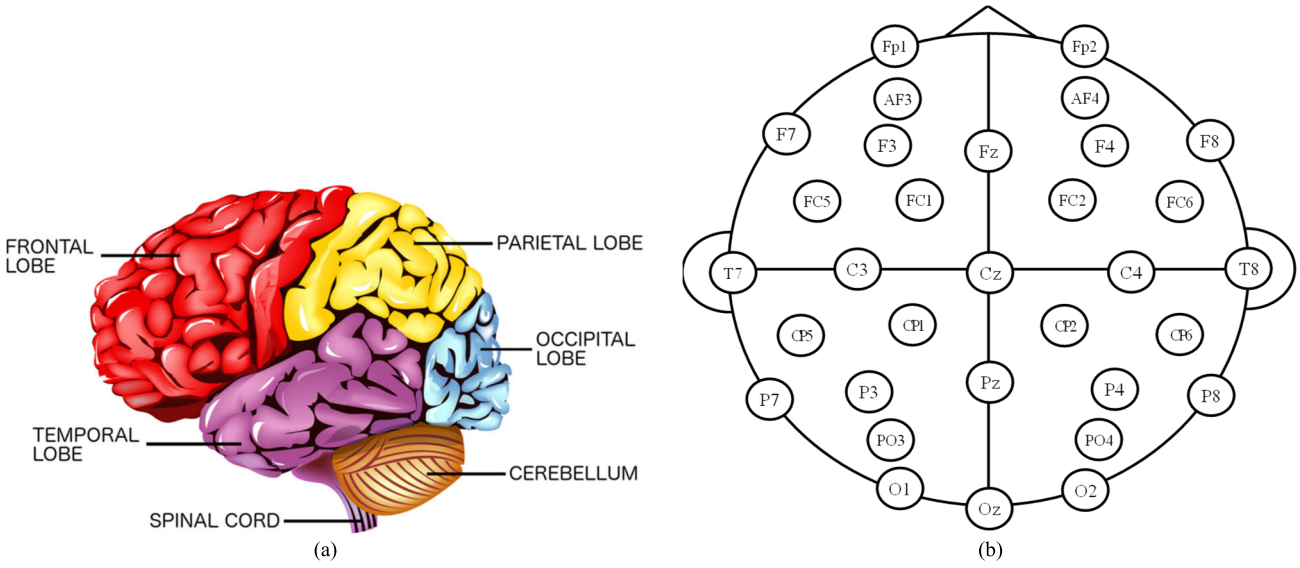

FIGURE 2. Standard 10/20 system sets of EEG electrodes locations on the skull: (a) Different parts of human brain [70]; (b) Electrodes for EEG recording in different lobes according to international 10/20 electrode placement system (for 32 channel EEG system).

3) SEGMENTATION

In order to increase samples for training, signal segmentation on four frequency bands (the three sub-bands and the full frequency spectrum of the EEG signals) is done. For this experiment, EEG signals are segmented using three sliding time windows, each with 50% overlap, as shown in Fig. 4. The window sizes are 4 seconds, 8 seconds, and 12 seconds. The descriptions of the three segmentations are given in Table 6.

As the sampling rate of the signal in the dataset 128Hz, so there are 512 (128 × 4), 1,024 (128 × 8), and 1,536 (128 × 12) data points in each segment of length 4-second, 8-second, and 12-second, respectively. Since each trial is 60 seconds long, so 29 segments are acquired using a time window of 4-second that moved every 2 seconds, 14 segments are obtained using a time window of 8-second that moved every 4 seconds, and 9 segments are obtained using a time window of 12-second that moved every 6 seconds. Finally, for a total

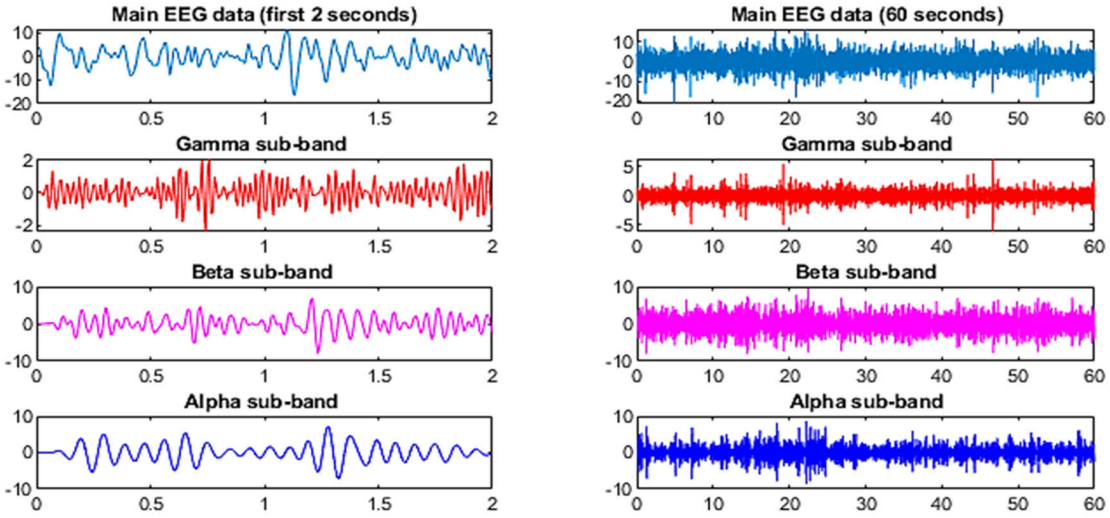

FIGURE 3. Main and sub-bands EEG signals of participant 1, video 1, channel 1.

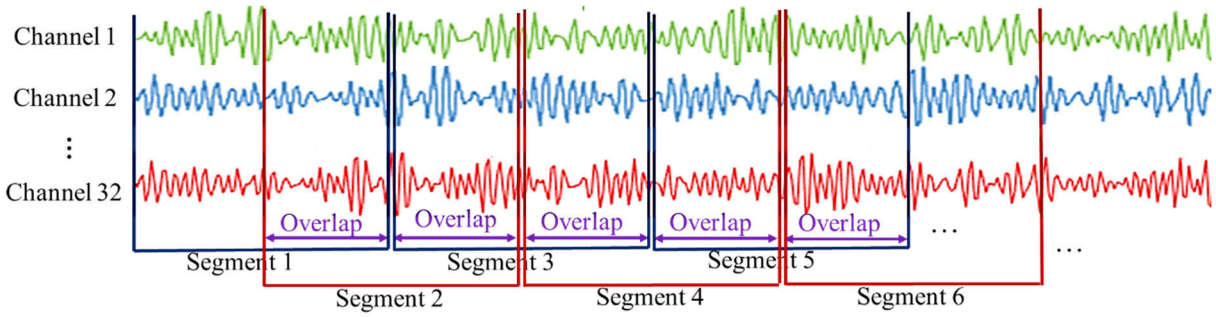

FIGURE 4. Illustration of segmentation with overlapping.

TABLE 4. File description for single participant in the pre-processed version of the dataset.

Array Name	Array Shape	Array Contents
data	40 × 40 × 8064	video/trial × channel × data
labels	40 × 4	video/trial × label (Valence, Arousal, Dominance, Liking)

of 32 participants, 37,120 (29 × 40 × 32), 17,920 (14 × 40 × 32), and 11,520 (9 × 40 × 32) samples are obtained using the 4-second, 8-second, and 12-second segmentation time windows, respectively.

4) DATASET ANNOTATION

The Valence-Arousal scale ranging from 1 (low) to 9 (high) is employed in this study to measure emotions. The scales are divided into two parts to construct this emotion recognition task (binary classification). Similar to the work in [8], Valence is divided into high (> 4.5) and low (≤ 4.5) according to the Valence scale and they are termed as HV and LV respectively; and Arousal is divided into high (> 4.5) and low ≤ 4.5) according to the Arousal scale and they are termed as HA and LA respectively.

TABLE 5. The channel layout in the pre-processed version of the dataset.

Channel No.	Channel Content	Channel No.	Channel Content	Channel No.	Channel Content	Channel No.	Channel Content
1	Fp1	9	CP5	17	Fp2	25	C4
2	AF3	10	CP1	18	AF4	26	T8
3	F3	11	P3	19	Fz	27	CP6
4	F7	12	P7	20	F4	28	CP2
5	FC5	13	PO3	21	F8	29	P4
6	FC1	14	O1	22	FC6	30	P8
7	C3	15	Oz	23	FC2	31	PO4
8	T7	16	Pz	24	Cz	32	O2

C. CONNECTIVITY FEATURE MAP (CFM) CONSTRUCTION

The feature extraction technique transforms inputs to new dimensions, which are different (linear, non-linear, directed, etc.) combinations of the inputs. Six types of connectivity measures are considered in this study for connectivity feature extraction and CFM construction. The strength of connectivity between two electrodes reflects the interaction between

two brain regions at single experiment. This interaction might be a direct correlation or inverse correlation, synchronization, or asynchronization, depending on cognitive or emotional activities. Relationships differ depending on the connectivity types as well. The connectivity methods chosen for this study are:

1) Linear functional connectivity methods: XCOR and its variant PCC.
2) Non-linear functional connectivity methods: PLV, MI and its variant NMI.
3) Non-linear effective connectivity methods: TE.

For each connectivity method, features are extracted from the three sub-bands and full frequency spectrum of the EEG signals. Therefore, there are four types of connectivity features for each connectivity method. There are three segmentation time windows for each frequency band. Thus, for eight in total, $6 \times 4 \times 3 = 72$ different types of connectivity features are extracted.

1) CROSS-CORRELATION (XCOR)

The XCOR function measures the linear correlation between two signals. The equation can also be written as:

$$XCOR_{XY}[l] = \begin{cases} \sum_{t=0}^{N-l-1} Xt + lYt & if\ l \geq 0 \\ XCOR_{YX}[-l] & if\ l < 0 \end{cases} \quad (1)$$

where $l = -(N-1), \ldots, -2, -1, 0, 1, 2, \ldots, (N-1)$. The variable l denotes a lag or time shift parameter, and $XCOR_{XY}[l]$ denotes the XCOR between two signals X and Y with lag l. For $l \geq 0$, signal $X(t)$ leads the signal $Y(t)$ by l positions, and for $l < 0$, $X(t)$ lags behind the signal $Y(t)$. If N is the finite length of the signals $X(t)$ and $Y(t)$, then the number of samples in the resultant XCOR sequence is $m = 2N - 1$. When $l = 0$, PCC is recovered [20].

Several features can be extracted from the XCOR sequence, such as mean or average, peak value, instant at which peak occurs, standard deviation, centroid, equivalent width, and mean square abscissa [72], [73]. The peak value of cross-correlation ($max(XCOR)$) is used in this study.

2) PEARSON CORRELATION COEFFICIENT (PCC)

PCC measures the linear correlation between two signals X and Y, which can be calculated as

$$PCC_{XY} = \frac{n\sum X_i Y_i - \sum X_i \sum Y_i}{\sqrt{n\sum X_i^2 - \left(\sum X_i\right)^2}\sqrt{n\sum Y_i^2 - \left(\sum Y_i\right)^2}}, \quad (2)$$

where n is the sample size, X_i, Y_i are the individual sample points indexed with i. The value of PCC ranges from -1 to 1, with a PCC of 0 indicating no linear dependence between the two signals, and a PCC of -1 or 1, respectively, denotes a complete linear inverse correlation or complete linear direct correlation between them.

3) PHASE LOCKING VALUE (PLV)

PLV expresses the phase synchronization between two signals, obtained as the average of the absolute phase differences, which is obtained as follows-

$$PLV_{XY} = \frac{1}{T}\left|\sum_{t=1}^{T} \exp\left\{j(\varphi_X^t - \varphi_Y^t)\right\}\right|. \quad (3)$$

Here, φ^t is the signal phase at time t, X and Y denote two electrodes, T is the signal time length. The value of PLV ranges from 0 to 1, where their limits indicate that the two signals are either entirely independent (0) or wholly synchronized (1), respectively.

4) MUTUAL INFORMATION (MI)

The amount of information about one random variable that may be learned from observing another is measured as MI. The following is the definition of MI between two random variables X and Y:

$$MI_{XY} = H(X) + H(Y) - H(X, Y). \quad (4)$$

In this case, H stands for Shannon entropy [74]. The marginal entropies of the two variables X and Y are $H(X)$ and $H(Y)$, respectively, and their joint entropy is $H(X, Y)$. MI is symmetric and nonnegative. The range of MI's value is $0 \leq MI_{XY} < \infty$. If MI_{XY} is equal to 0, then X and Y are independent. If MI_{XY} is greater than 0, then X and Y are dependent.

5) NORMALIZED MI (NMI)

As MI_{XY} does not typically have definite upper bounds, it is sometimes better to normalize this measure such that $MI_{XY} \in [0, 1]$. In NMI, MI_{XY} is normalized by $H(X) + H(Y)$ to provide a value between 0 (independence) and 1 (strong dependence), with the equation being written as:

$$NMI_{XY} = \frac{H(X) + H(Y) - H(X, Y)}{H(X) + H(Y)} = 1 - \frac{H(X, Y)}{H(X) + H(Y)}. \quad (5)$$

6) TRANSFER ENTROPY (TE)

TE measures the directed flow of information from a time series or signal Y to another signal X. In other words, it describes the gain obtained by knowing Y for the prediction of X.

$$TE_{Y\to X} = H(X_t, Y_t) - H(X_{t+h}, X_t, Y_t) + H(X_{t+h}, Y_t) - H(X_t). \quad (6)$$

Here, X_{t+h} is the future of X_t and $h = 1$ is chosen for this study. If $X_{t+h} = w$, then $TE_{Y\to X}$ can be computed as a combination of entropies:

$$TE_{wXY} = H(w, X) + H(X, Y) - H(X) - H(w, X, Y). \quad (7)$$

The range of TE value is $0 \leq TE_{Y\to X} < \infty$. If $TE = 0$, then there is no causal relationship between the two time series. $TE \geq 0$ indicates that, a causal relationship exists between the two time series.

For calculating the probability that is required to calculate entropy, the fixed bin histogram approach is followed. Sturges' Rule is followed to select the number of bins. If n is the number of data points in each segment, 'Sturges' rule uses the following formula to determine the optimal number of bins to use in a histogram:

$$\text{Number of bins} = \lceil \log_2 n + 1 \rceil . \tag{8}$$

In the case of CFM, the variables are signals from individual EEG channels. The connectivity features are computed for every pair (X, Y) of EEG channels. Consequently, if there are N channels, the number of obtained features is $N(N-1)/2$ for undirected connectivity and $N(N-1)$ for directed connectivity. The connectivity features for all channel pairs can be represented in a matrix (i.e., CFM) as shown in Fig. 5. The CFMs have 32 rows and 32 columns for 32 EEG channels. Thus, the size of each connectivity matrix is 32×32. The element of the matrix at position (X, Y) specifies the connectivity between the EEG signals found from the Xth and Yth channels. The CFM is equivalent to the adjacency matrix of a graph in which the EEG channels are considered as nodes and the connectivity features as edge weights.

D. EMOTION CLASSIFICATION USING CONVOLUTIONAL NEURAL NETWORK (CNN)

Among different DL methods, CNN is the most successful classifier for 2D data and can implicitly extract relevant features [75]. Since the constructed CFMs are in 2D, CNN is chosen as a suitable classifier. In general, a CNN architecture consists of an input layer, several convolutional-subsampling layers, flatten layer, a fully connected layer, and an output layer. The first operation of a CNN is convolution performed on the input (matrix, image, or map) with its kernel, which generates a new convolved matrix. Preceding subsampling operation will downsize the convolved matrix with important features. After one or more convolutional-subsampling operations through a fully connected dense layer, the output layer categorizes the given 2D matrix as input of the CNN.

Three convolutional layers, two max-pooling layers, flatten layer, a dense layer, and an output layer make up the CNN architecture employed in this study. Fig. 6 depicts the CNN architecture used in this study. Every convolution layer used kernels of size 3×3, and the stride is set to 1. Rectified linear unit (ReLU) is used as an activation function. The numbers of filters are 32, 64, and 128 for the 1st, 2nd, and 3rd convolution layers, respectively. The same convolution (i.e., padding $= 1$) is used for all the convolution layers to preserve the information of the corner pixels of the input feature map. Fig. 6 clearly shows how many filters, strides, and padding are included in each layer. Two max-pooling layers are used; one is after the 1st convolution layer and another is after the 3rd convolution layer. Every pooling layer uses kernels whose size is 2×2 with stride 2. After each max-poling layer, batch normalization is used to accelerate the model training. After convolution and pooling operation, the feature map is flattened to a single-column vector and fed to the dense layer. The dense layer and output layer's respective neuron counts are set at 128 and 2, respectively, and the dense layer is accompanied by a 25% dropout to minimize overfitting. In the output layer, the ''Sigmoid'' activation function is applied.

IV. EXPERIMENTAL STUDIES

This section describes the experimental outcomes of the ER system for CMFs created with XCOR, PCC, PLV, MI, NMI, and TE individually. The efficacy of these methods is assessed based on the test set recognition accuracies.

A. EXPERIMENTAL SETUP AND EVALUATION METRIC

The CNN is trained by the Adam algorithm [74], and binary cross-entropy is used as the loss function. The learning rate, batch size, and epochs for the CNN are set to 0.00001, 32, and 500. A 5-fold Cross Validation (CV) is applied, where 20% of the available data are reserved as testing set by turn. We also considered the Training–Test split as 80% and 20%. Two DL frameworks, Keras and Tensorflow, available in Python, are used for implementing the CNN model for the classification process. The P100 GPU in the Kaggle platform was used for training the model, and MATLAB R2021a was used for feature extraction through the device of configuration: CPU: Intel(R) Core(TM) i5-4200 CPU @ 2.50 GHz, RAM: 4.00 GB, 64-bit windows operating system.

The performance of the model is evaluated using widely used evaluation metric named accuracy, precision, recall (i.e., sensitivity and specificity), and F1 score. Accuracy can be calculated using Equation 9. For HV or HA class, precision (Pr^+), recall (Rc^+), and F1 score (F1^+) are sown in Equation 10-12. Similarly, for LV or LA class, Pr^-, Rc^- (i.e., specificity), and F1^- are also calculated.

$$Accuracy = (TP + TN)/(TP + TN + FP + FN) \tag{9}$$

$$Pr^+ = TP/(TP + FP) \tag{10}$$

$$Rc^+ \text{or } Sensitivity = TP/(FN + TP) \tag{11}$$

$$F1^+ = (2 \times Pr^+ \times Rc^+)/(Pr^+ + Rc^+) \tag{12}$$

Here, TP or true positive means the samples are labelled originally as high, and the model also predicted those as high. TN or true negative means the samples are labelled originally as low, and the model also predicted those as low. FP or false positive means the samples are labelled originally as low, but the model predicted those as high. FN or false negative means the samples are labelled originally as high, but the model predicted those as low. Since only accuracy metrics can't show the effectiveness of deep learning models for classification, the other performance measures are used for extensive study. For example, the precision score (Pr^+) shows the model's ability to avoid the false-positive measure whereas the recall score (Rc^+) signifies the model's ability to correctly predict the positives out of actual positives. F1 score (F1^+) is a representation of accuracy giving equal weight to both the precision and recall.

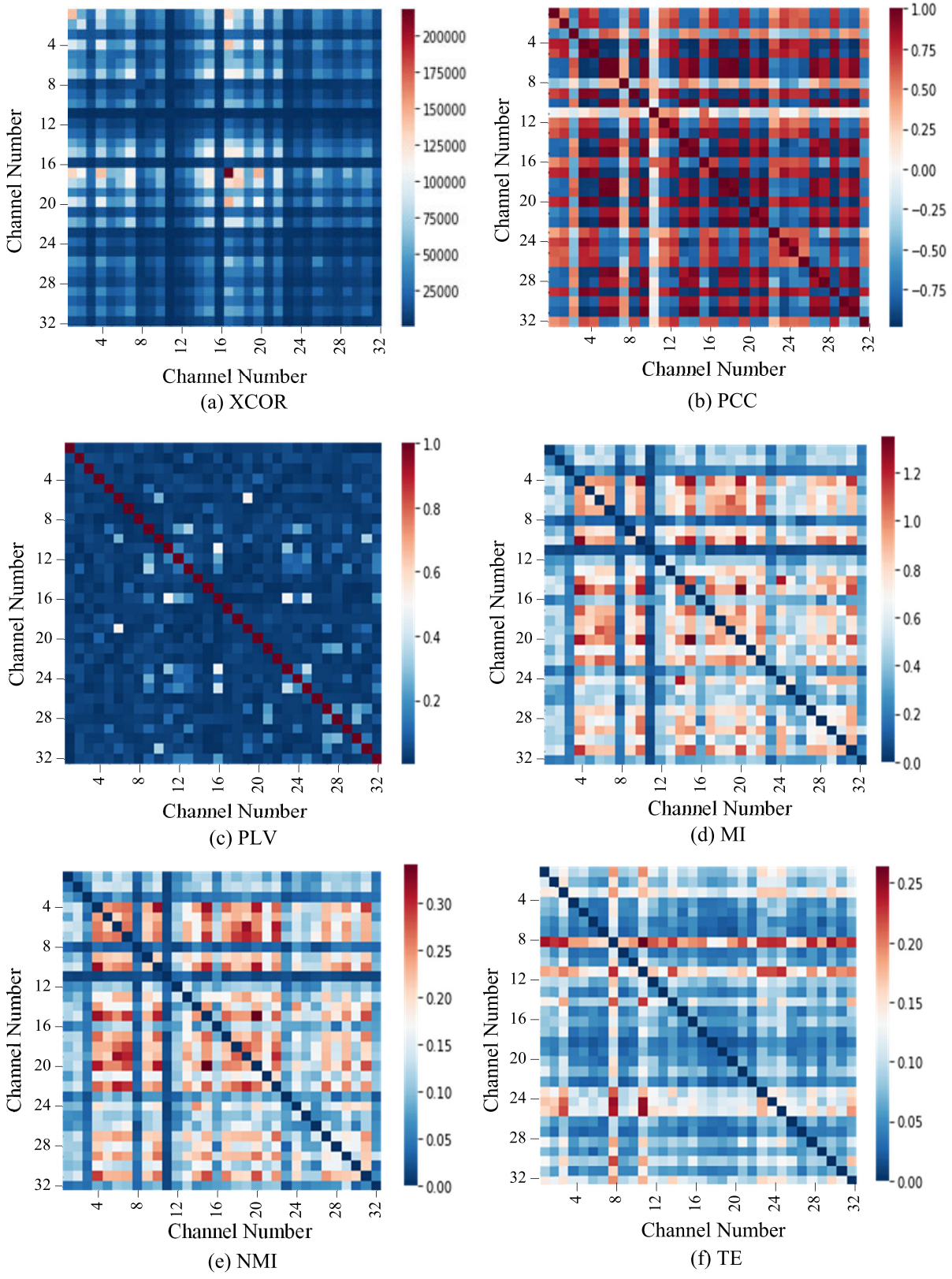

FIGURE 5. Sample connectivity feature map (CFM) constructed with different methods.

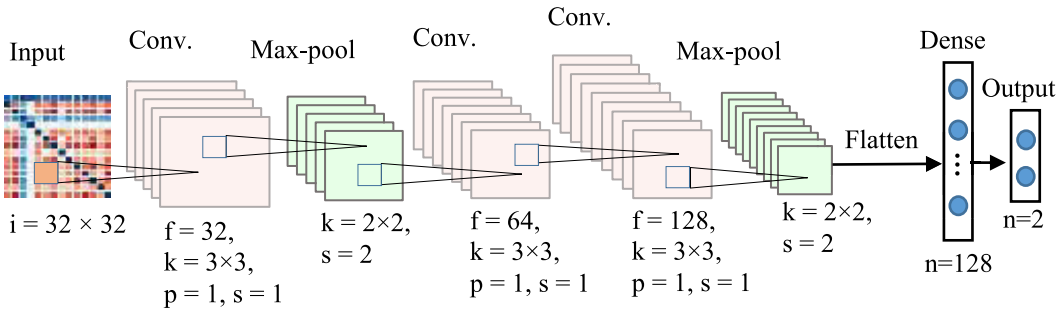

i = Input Size; f = Numbers of Filters; k = Kernel Size; p = Padding; s = Stride; n = Numbers of Neurons.

FIGURE 6. Configuration of the CNN model for emotion recognition used in this study.

B. EXPERIMENTAL RESULTS

In the experiment, the connectivity features are compared with respect to their accuracy and time. The accuracies are calculated for four different frequency bands (Alpha, Beta, Gamma, and full frequency) with three different segmentation time windows. The time required to construct CFM with individual connectivity methods is calculated for the three different segmentation time windows. The training time varying segmentation time windows are also calculated.

1) PERFORMANCE COMPARISON

Firstly, the model's loss and accuracy curves are compared for the Gamma frequency band and full EEG signals. Then, the classification accuracy, specificity, sensitivity, precision and F1 score have been compared. The results are for 8-second segmentation frame. Finally, the overall classification results of all connectivity methods for all three sub-frequency bands and for the full frequency spectrum are presented in two modes (5-fold CV and training-test split) for all three segmentations.

The model loss and accuracy curves for Valence and Arousal classification with a data length of 8 seconds are shown in Fig. 7-Fig. 8 for the Gamma frequency band. From Fig. 7(a) and Fig. 8(a), it can be seen that the loss convergence of the model for TE is slightly faster than the other feature and the loss convergence for PCC and XCOR are slower. Faster convergence indicates that the model can easily learn these features. Similar characteristics can also be found in Fig. 7(b) and Fig. 8(b), where the accuracy improvement is faster for TE, followed by MI, NMI, PLV, and PCC, and the accuracy improvement for XCOR is slower among all the methods. According to Fig. 7(c) and Fig. 8(c), the accuracy for MI-based connectivity is higher than that of others. The accuracies of PCC and PLV are competitive and less than that of MI-based features. The results obtained from effective connectivity TE are less than functional connectivity (e.g., PCC, PLV, and MI), though effective connectivity containing the directional information. The best result achieved in this study is with the NMI feature.

The classification performance of the models in a train-test split mode that used different features in the Gamma frequency band is shown in Table 7. The table contains the accuracy of individual classes of low and high (i.e., specificity and sensitivity), precision, F1 score for both Valence and Arousal and the overall accuracy of the classification. From Table 7, it can be observed that the NMI method achieved higher specificity, sensitivity, and accuracy in both Valence and Arousal classification. The precision and F1 score are also found better or comparable for NMI connectivity.

TABLE 6. Descriptions of different segmentation.

Segmentation time window	Overlapping	No. of segment in a trial	Total no. of segments (no. of seg. in a trial × 40 × 32)	No. of data-point in a segment (seg. time window × 128)
4s	2s	29	37,120	512
8s	4s	14	17,920	1,024
12s	6s	9	11,520	1,536

Similar to the Gamma frequency band, the loss convergence of the model for the TE feature is faster than all other features also in the full frequency spectrum of the signals, as seen in Fig. 9(a) and Fig. 10(a), and accuracy improvement in Fig. 9(b) and Fig.10(b). There is a slow start in decreasing the loss and improvement in accuracy for PLV. According to Fig. 9(c) and Fig. 10(c), the overall accuracy in the full frequency spectrum is less than that of Gamma band. For PLV, the test accuracy starts to increase, and after a few epochs, the accuracy decreases both for Valence and Arousal.

The classification performance of the models in train-test split mode that used different features in the full frequency spectrum of the signals is shown in Table 8. The table contains the accuracy of individual classes of low and high (i.e., specificity and sensitivity), precision, F1 score for both Valence and Arousal and the overall accuracy of the classification. The results are obtained with a signal length of 8 seconds from the full frequency spectrum. Table 8 identified that the results of the classification in the full frequency band are similar manner as the results in the Gamma frequency band.

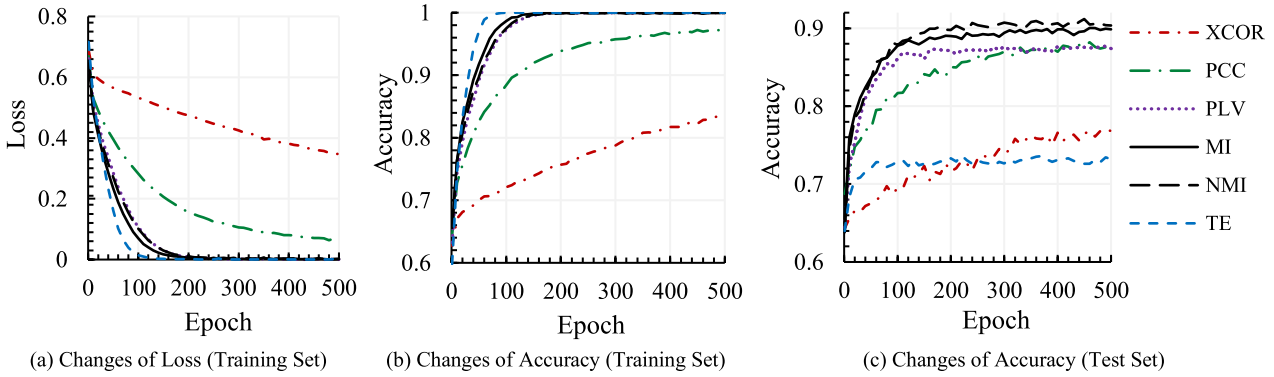

(a) Changes of Loss (Training Set) (b) Changes of Accuracy (Training Set) (c) Changes of Accuracy (Test Set)

FIGURE 7. Model loss and accuracy for valence classification using data with length of 8 seconds (gamma band).

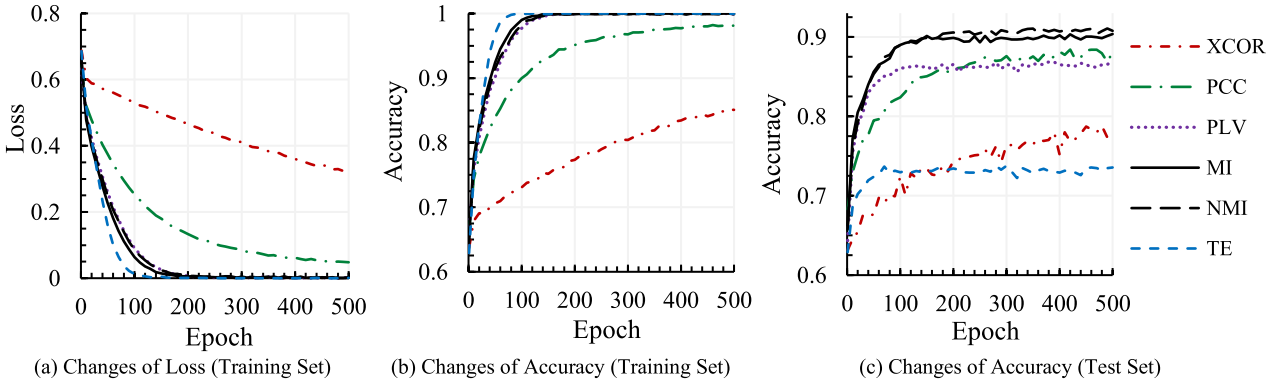

(a) Changes of Loss (Training Set) (b) Changes of Accuracy (Training Set) (c) Changes of Accuracy (Test Set)

FIGURE 8. Model loss and accuracy for arousal classification using data with length of 8 seconds (gamma band).

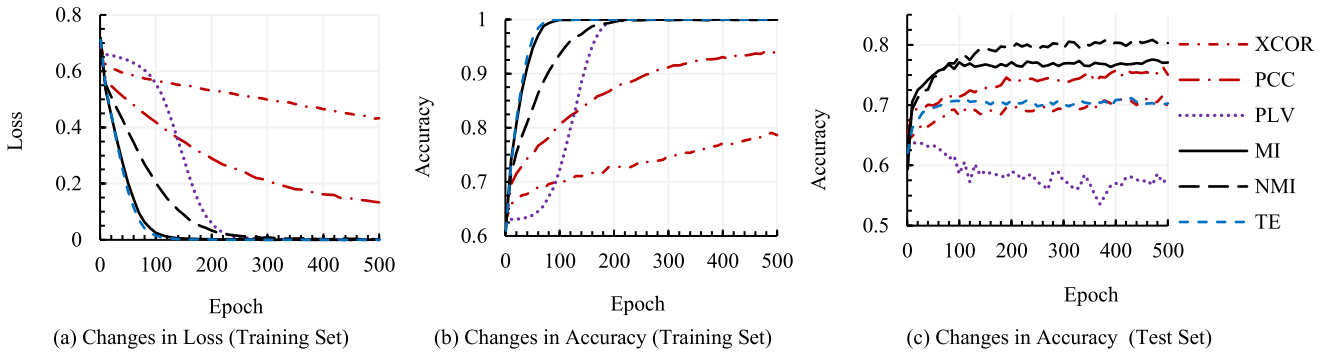

(a) Changes in Loss (Training Set) (b) Changes in Accuracy (Training Set) (c) Changes in Accuracy (Test Set)

FIGURE 9. Model loss and accuracy for valence classification using data with length of 8 seconds in full frequency spectrum.

In both Valence and Arousal classification, NMI achieved higher specificity, sensitivity, and accuracy than the other connectivity methods. The precision and F1 score are also found better or comparable for NMI connectivity.

The results of the Valence and Arousal classification in training-test split mode with different connectivity methods in four different frequency bands are shown in Fig. 11. The results are obtained from the data segmented with a time window of 8 seconds. As mentioned earlier, it is reported in the literature that the sub-bands may yield more accurate information about constituent neuronal activities [11] and emotion is highly related with Beta and Gamma sub-band and moderately related with Alpha sub-band. The obtained results of this study also satisfy this observation on frequency band compatibility for emotion recognition. We observed that the recognition accuracy is higher in sub-bands more specifically in Gamma sub-band rather than the other bands or full EEG. Among all the connectivity methods, NMI achieved higher accuracies in all four frequency bands.

Table 9 presents the test set accuracies on Valence and Arousal classifying CFMs constructed by different feature extraction methods for the Alpha, Beta, Gamma bands, and

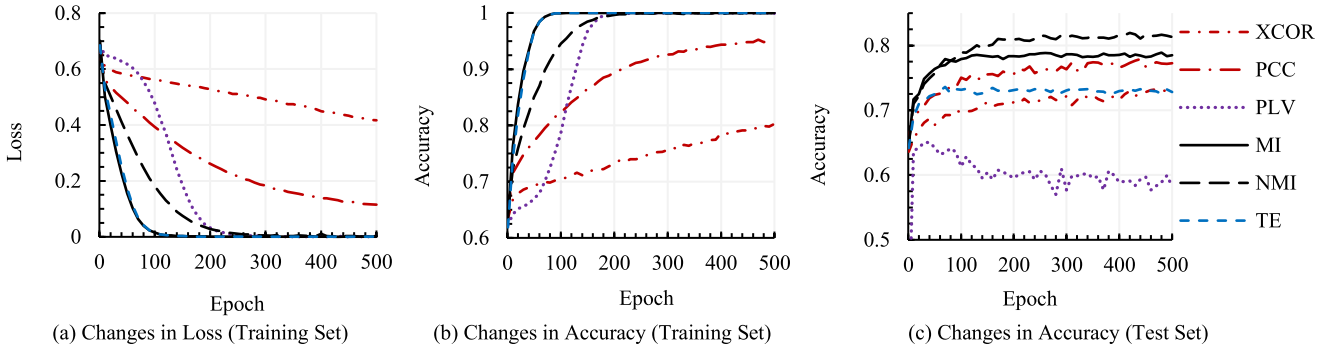

(a) Changes in Loss (Training Set) (b) Changes in Accuracy (Training Set) (c) Changes in Accuracy (Test Set)

FIGURE 10. Model loss and accuracy for arousal classification using data with length of 8 seconds in full frequency spectrum.

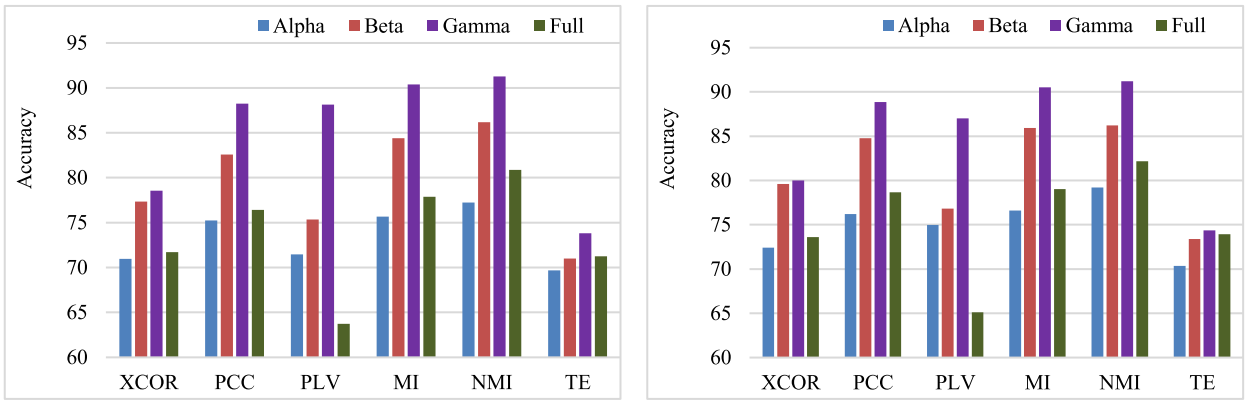

(a) Valence (b) Arousal

FIGURE 11. Results valence and arousal classification in training-test split mode with different connectivity methods in different frequency bands with data length of 8 seconds.

TABLE 7. Performance comparison of different CFM methods in train-test split mode with signal length of 8 seconds from the gamma frequency band.

			XCOR	PCC	PLV	MI	NMI	TE
Valence	Accuracy (%)		78.54	88.25	88.14	90.40	91.26	73.80
	Sensitivity (%)		88.02	92.57	90.67	93.01	93.94	89.96
	Specificity (%)		62.30	80.84	83.80	85.91	86.67	46.10
	Precision (%)	LV	75.22	86.40	83.99	87.78	89.31	72.84
		HV	80.00	89.22	90.55	91.88	92.35	74.09
	F1 Score (%)	LV	68.15	83.52	83.89	86.87	87.97	56.46
		HV	65.09	90.86	90.60	92.44	93.13	81.25
Arousal	Accuracy (%)		79.99	88.87	87.00	90.54	91.21	74.36
	Sensitivity (%)		90.02	92.77	90.41	93.30	95.05	91.37
	Specificity (%)		62.35	81.98	80.98	85.68	84.44	44.41
	Precision (%)	LV	78.03	86.58	82.76	87.91	90.66	74.54
		HV	80.79	90.05	89.32	91.97	91.49	74.30
	F1 Score (%)	LV	69.31	84.21	81.86	86.78	87.43	55.65
		HV	85.15	91.38	89.68	92.63	93.23	84.95

full frequency spectrum signals. Results presented for the three different segmentation time windows (i.e., 4 seconds, 8 seconds, and 12 seconds) having 50% overlap. The best results for each individual connectivity method are marked as bold for ease of interpretation of the results. Both 5-fold CV and 80%-20% training-test sets split for training CNN performance measure are presented for better observations. For segmentation time window variations, generally, 8s and 12s are fond competitive and better than 4s. Therefore, the following discussions are for 5-fold CV with 8s time window for all the cases.

It is observed from Table 9 that the performance of functional connectivity methods (e.g., PCC, MI) is comparatively better than the effective connectivity method (i.e., TE).

As an example, XCOR shows an accuracy of 76.89% for Valance classification with the Gamma band, whereas, for the same Gamma band, TE shows 73.22% accuracy. Among all the connectivity methods, TE achieved the lowest accuracy. Among the functional connectivity methods, non-linear connectivity methods (e.g., MI) performed better than linear connectivity methods (e.g., PCC), according to the results presented in Table 9. Between linear connectivity methods, PCC is generally better than XCOR. As an example, PCC obtained an accuracy of 87.47% for Valance classification with the Gamma band, whereas, for the same Gamma band, XCOR showed 76.89% accuracy. Among the non-linear connectivity methods, any MI-based method (i.e., MI or NMI) performed better than PLV. For example, 89.98% accuracy is achieved through the MI feature, while PLV achieved 87.56% for Valence classification in the Gamma frequency band. Between the two MI- based methods, NMI is better than MI. For instance, NMI achieved 90.75% for Valence and 90.83% for Arousal, while MI achieved 89.98% for Valence and 90.14% for Arousal.

The ER accuracy concerning the Arousal dimension is higher than that of the Valence dimension in most of the cases, as seen in Table 9. For example, PCC, a functional connectivity method, shows an accuracy of 81.86% for Valence and 83.68% for Arousal in the Gamma frequency band. Similarly, TE, an effective connectivity method, achieved 73.22% for Valence and 73.65% for Arousal in the Gamma frequency band. For both PCC and TE, a similar scenario is observed for other frequency bands. Among all the eight connectivity methods and four frequency bands, only PLV in the Gamma band and PMI in the Beta band achieved higher accuracy in the Valence dimension (87.56% for PLV and 86.81% for PMI) than that of Arousal (86.55% for PLV and 86.50% for Arousal) dimension.

The higher frequency bands are more suitable for ER for each connectivity method, as shown in Table 9. Three sub-frequency bands are used with each connectivity method; Alpha (8–12 Hz), Beta (13–29 Hz), and Gamma (30–50 Hz). For all the connectivity methods, it is observed from the table that the Gamma band provides higher classification accuracies than the other two sub-frequency bands and the full frequency of the signals for both Valence and Arousal. Results from the Beta band are lower than the Gamma band, and the Alpha band has shown the worst performance. For example, NMI achieved 76.64%, 85.54%, and 90.75% in Valence classification for the frequency bands Alpha, Beta, and Gamma, respectively. According to the presented results in Table 9, the NMI, a variant of MI, is the most effective in terms of accuracy. At a glance NMI is the best-suited CMF method for ER, which is significant outcome of the present study.

2) FEATURE EXTRACTION AND TRAINING TIME COMPARISON

Table 10 presents the time required to extract the feature with the three segmentation time windows (i.e., 4 seconds, 8 seconds, and 12 seconds) for different connectivity methods. The feature extraction time is calculated in two different manners. The time needed to contract a CFM and time to construct the total CFM for one trial (i.e., a 60-second video). As the numbers of both trials and participants are the same for each connectivity method, a single trial is used to compare time. The required time to train the model in different segmentation time windows is also presented in Fig. 12.

From Table 10 it can be observed that the time needed for feature extraction varies with the connectivity methods. Among the connectivity methods, MI, NMI, and TE require a relatively higher time for feature extraction than that of XCOR, PCC, and PLV. The time needed to construct a CFM for the data length of 8 seconds with XCOR, PCC, and PLV are 0.26 seconds, 0.02 seconds, and 0.06 seconds, respectively, while MI, NMI, and TE require 0.85 seconds, 0.91 seconds, and 1.27 seconds, respectively. Among all the connectivity methods, PCC requires the lowest time, and TE requires the highest time for feature extraction.

The feature extraction time also varies with the segmentation time window. In the shorter segment, the numbers of data points are low, thus requiring less time to construct a CFM. But, with a shorter segmentation time window, the numbers of total CFMs get increased, which requires more time than a longer segment with fewer numbers of CFM. For example, TE requires 1.16 seconds and 1.27 seconds to construct a CFM with a data length of 4 seconds and 8 seconds, respectively. There are $4 \times 128 = 512$ data points in 4 seconds segment and $8 \times 128 = 1{,}024$ data points in 8 seconds segment, and computation requires more time for more data points. If a complete trial is considered, there are 29 CFMs and 14 CFMs for 4 seconds and 8 seconds time windows, each with 50% overlap, and these require 20.86 seconds and 11.89 seconds, respectively, for the TE method. These similar scenarios can be observed for each connectivity method and for all three segmentation time windows.

The times are displayed for training up to 100 epochs with XCOR feature in Fig. 12. According to the figure, the time required to train the model vary with the numbers of inputs, i.e., CFMs. The model took higher time to be trained when the numbers of CFMs get increased. With shorter time window, the numbers of CFMs increased and thus require larger training time. For example, in case of XCOR, the model took 325.66 seconds with 29,696 CFMs (i.e., 80% of 37,120) and 161.67 seconds with 14,336 CFMs (i.e., 80% of 17,920) to be trained, where the segmentation lengths are 4 seconds and 8 seconds, respectively, which are displayed in Fig. 12.

3) COMPARISON WITH EXISTING STUDIES

Table 11 compares the Valence and Arousal classification accuracies obtained in this study with other ER studies on the DEAP dataset. The table also shows the length of the segmentation time window with overlapping, classification, and validation methods. The best result for each connectivity method is written in bold. From the table, it can be observed that classification accuracies vary with segmentation time

TABLE 8. Performance comparison of different CFM methods in training-test split mode with signal length of 8 seconds from the full frequency spectrum.

			XCOR	PCC	PLV	MI	NMI	TE
Valence	Accuracy (%)		71.70	76.42	63.75	77.87	80.88	71.26
	Sensitivity (%)		89.35	93.94	83.51	90.36	94.87	89.65
	Specificity (%)		41.48	46.40	29.90	56.47	56.92	39.74
	Precision (%)	LV	69.45	81.73	51.43	77.38	86.63	69.16
		HV	72.34	75.01	67.11	78.05	79.05	71.82
	F1 Score (%)	LV	51.93	59.19	37.81	65.29	68.70	50.47
		HV	79.95	83.41	74.41	83.75	86.24	79.75
Arousal	Accuracy (%)		73.60	78.68	65.12	79.04	82.19	73.93
	Sensitivity (%)		86.38	90.37	83.50	94.66	94.44	89.80
	Specificity (%)		51.11	58.12	32.79	51.57	60.66	46.03
	Precision (%)	LA	68.10	77.43	53.05	84.59	86.12	71.96
		HA	75.66	79.14	68.60	77.47	80.85	74.53
	F1 Score (%)	LA	58.39	66.39	40.52	64.07	71.18	56.14
		HA	80.66	84.38	75.32	85.20	87.11	81.45

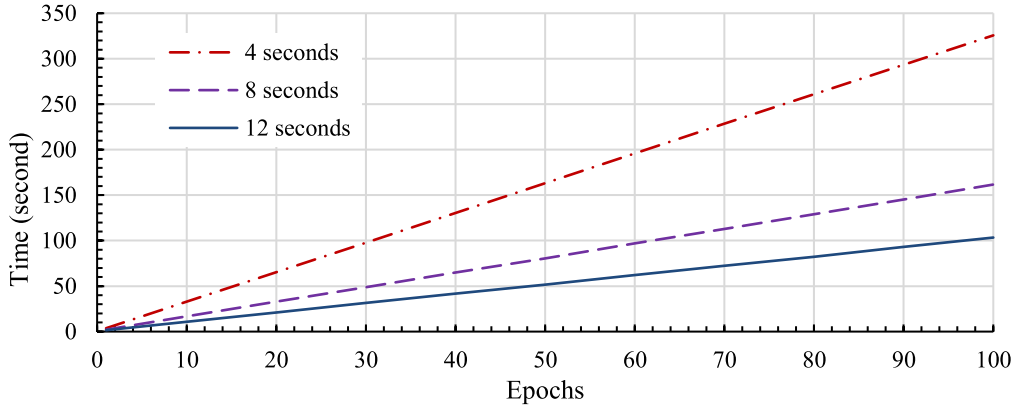

FIGURE 12. Time comparison of different segmentation sizes in training the model.

and overlapping, classifier and also with validation method. For PCC, the best accuracy was achieved by the study [21], where segment overlapping is about 83% with CNN classifier in 5 Fold CV mode. But the study [8] also used CNN as a classifier and same segmentation time window but without overlapping, and the accuracy reduces. The study [16] used CNN to classify emotion with two segmentation time windows with different overlapping. The segmentation time window is longer than that of the above-mentioned two studies. Overlapping of 50% and 66% were used with segmentation lengths of 8s and 12s, respectively and achieved accuracies higher than the study [8] but lower than the study [21]. The accuracy improved when a hybrid classification model was used. The study [16] shows that accuracy reduces with a longer segmentation time window. The lowest accuracies were achieved by the study [46], where SVM was used for classification without segmentation. This study used CNN classifier with a segmentation length of 8s and the overlapping is 50%, which is the same as the study [16] and achieved accuracies of 88.25% and 88.87% for Valence and Arousal, respectively, with PCC that is higher than the study of [16].

The best results achieved in this study are with NMI feature, 91.26% for Valence and 91.23% for Arousal, which are better than the traditional ML-based study [51], [55], [46] and have shown competitive performance with a recent study [21], [23] with other different connectivity features and DL methods. For Valence classification, the study [21] achieved higher accuracy, and for Arousal classification, the study [23] achieved higher accuracy with the PLV feature. This study with the NMI feature has shown superior to the recent DL-based study [16], [8], where CNN is used as a classifier, and PCC is used as a feature. Finally, the ER system with NMI and CNN is a good EEG-based ER system.

V. DISCUSSION

In recent years, ER has achieved significant development, and connectivity methods are widely used for feature extraction. In this investigation-type research, 2D feature maps from EEG signals using the prominent connectivity measures have been examined as efficient input of DL-based classifiers targeting higher accuracy in emotion recognition. More emphases have been placed on in-depth analysis from various directions methodically to find the prominent feature map from popular connectivity feature extraction methods where some of the analyses and verification strategies are computation time consideration besides accuracy/loss and other com-

TABLE 9. Classification comparison using different CFM methods.

CFM Method	Frequency Band	Test Set Accuracy (%)											
		5 Fold Cross Validation						Training-Test Sets Split as 80%-20%					
		Valence			Arousal			Valence			Arousal		
		4s	8s	12s	4s	8s	12s	4s	8s	12s	4s	8s	12s
XCOR	Alpha	68.28	68.66	70.29	70.54	71.32	71.83	68.96	70.98	71.26	71.75	72.40	72.39
	Beta	75.86	76.16	75.50	77.79	78.56	79.27	75.95	77.34	75.56	78.25	79.60	80.03
	Gamma	76.95	76.89	74.93	79.62	78.24	78.40	78.25	78.54	75.69	80.15	79.99	79.64
	Full Frequency	70.70	71.07	69.61	73.27	72.26	71.40	69.58	71.70	71.70	71.55	73.60	71.91
PCC	Alpha	72.27	74.18	76.36	74.44	75.42	77.19	72.68	75.25	77.38	74.94	76.22	77.90
	Beta	81.25	81.86	83.02	82.52	83.68	84.08	81.58	82.58	83.55	83.17	84.79	84.80
	Gamma	86.66	87.47	86.68	87.47	88.17	88.00	87.31	88.25	87.15	87.75	88.87	88.84
	Full Frequency	75.78	75.80	76.22	77.75	77.51	77.56	76.49	76.42	76.60	78.44	78.68	78.34
PLV	Alpha	68.46	70.03	73.09	69.90	74.17	74.24	68.85	71.45	73.78	71.21	74.97	76.12
	Beta	70.40	74.77	75.91	72.72	75.88	77.30	71.88	75.36	77.12	73.90	76.84	77.95
	Gamma	84.33	87.56	88.33	85.19	86.55	87.90	84.71	88.14	88.80	85.62	87.00	88.75
	Full Frequency	63.32	62.66	62.43	63.97	64.21	64.34	63.40	63.75	63.19	64.22	65.12	65.84
MI	Alpha	73.74	74.75	77.31	75.94	76.03	79.21	74.12	75.66	77.90	76.45	76.61	80.25
	Beta	81.68	84.14	85.84	82.07	85.47	86.97	81.89	84.40	86.58	82.50	85.93	87.36
	Gamma	87.45	89.98	90.29	88.58	90.14	90.43	87.95	90.40	90.75	88.82	90.54	91.01
	Full Frequency	78.07	77.07	79.55	79.94	78.61	81.50	78.52	77.87	80.03	80.30	79.04	82.42
NMI	Alpha	74.31	76.64	77.57	77.31	78.78	80.60	74.72	77.23	78.21	78.01	79.21	81.20
	Beta	82.62	85.54	85.98	84.60	85.75	87.56	83.17	86.18	86.45	84.93	86.24	87.97
	Gamma	88.84	90.75	90.20	90.38	90.83	90.68	89.28	91.26	90.71	90.82	91.21	91.23
	Full Frequency	78.32	80.42	79.67	82.30	81.39	82.61	78.85	80.88	80.29	82.92	82.19	82.98
TE	Alpha	65.03	69.01	70.05	70.31	69.74	70.80	65.90	69.67	71.18	71.03	70.34	71.78
	Beta	69.50	70.31	71.94	71.25	72.79	74.14	70.42	71.01	72.39	71.67	73.38	74.65
	Gamma	71.80	73.22	74.95	73.72	73.65	75.30	72.57	73.80	75.52	74.46	74.36	75.86
	Full Frequency	69.81	70.26	73.94	72.62	72.94	74.03	70.56	71.26	74.60	73.57	73.93	74.47

TABLE 10. Time comparison of the CFM methods in feature extraction.

CFM Method	Required Feature Extraction Time in Second						
	To Construct a Single CFM			To Construct CFMs for a Trial			To Construct CFMs for a Single Subject and Total Dataset
	4s	8s	12s	4s	8s	12s	
XCOR	0.18	0.26	0.36	3.56	2.53	2.29	Time for a Subject = Time for Trial × 40
PCC	0.01	0.02	0.03	0.28	0.25	0.24	Time for Total Dataset = Time for Trial × 40 × 32
PLV	0.03	0.06	0.08	1.02	0.90	0.81	
MI	0.75	0.85	0.94	13.13	7.34	5.64	
NMI	0.76	0.91	0.94	13.21	7.45	5.72	
TE	1.16	1.27	1.46	20.86	11.89	9.15	

mon performance measures, frequency band superiority analysis. A customized CNN model has been used as classifier for the emotions recognition task. Besides, the importance of the gamma band of EEG has been analyzed and its superiority is verified through experimental results and literature surveys. Higher classification accuracy is achieved in this study in the Gamma band using NMI connection features.

A. DISCUSSION ON PERFORMANCE OF DIFFERENT METHODS

This study investigates several prominent connectivity methods with their variants for feature extraction from EEG signals for ER. The connectivity features are selected from different categories, such as linear and non-linear functional and effective connectivity, where functional connectivity methods are found to be better than effective connectivity methods, and non-linear functional connectivity methods are better than linear functional connectivity methods.

The accuracy of PCC and PLV is less competitive than that of MI-based features. These results are consistent with the findings of the study [46], where MI was identified as the most informative connectivity measure. In the study [46], three functional connectivity, PCC, PLV, and MI, were used individually for ER. The best accuracy achieved with MI and the results obtained from PCC and PLV were competitive. Though the study [46], used SVM for classification, the same scenarios are also observed in this study, where CNN is used for classification. The results obtained from TE are less than that of other connectivity methods (e.g., PCC, PLV, and MI) though TE contains the directional information. These results are also consistent with the study [23] and [7], where PCC, PLV, and TE were used for emotion recognition and emotional video classification, respectively. The results obtained in the study [23] and [7], from TE features were less than those obtained from PCC and PLV.

TABLE 11. Performance comparison with other studies on the DEAP dataset.

CFM Method	Classifier and Ref.	Training-Test Split / Cross Validation	Segmentation Time Window (Overlapping)	Accuracy (%)	
				Valence	Arousal
XCOR	CNN (Current Study)	80% - 20%	8s (4s) for Valence, 4s (2s) for Arousal	78.54	80.15
PCC	SVM [46]	Leave 01 Trial Out	No Segmentation	72.91	72.34
	CNN [8]	90% - 5% - 5%	3s (0s)	78.22	74.92
	CNN [21]	5 Fold CV	3s (2.5s)	**94.44**	-
	CNN + SAE + DNN [16]	80% - 20%	12s (8s)	82.16	85.47
			8s (4s)	89.49	92.86
	CNN [16]	80% - 20%	12s (8s)	75.13	76.12
			8s (4s)	78.80	82.25
	CNN (Current Study)	80% - 20%	8s (4s)	88.25	88.87
PLV	SVM [46]	Leave 01 Trial Out	No Segmentation	73.75	71.88
	CNN [21]	5 Fold CV	3s (2.5s)	**99.72**	-
	DARCNN [23]	10 Fold CV	3s (2.5s)	95.15	**94.84**
		Leave 01 Subject Out	3s (2.5s)	88.28	87.60
	CNN (Current Study)	80% - 20%	12s (6s)	88.80	88.75
MI	SVM [46]	Leave 01 Trial Out	No Segmentation	76.17	73.59
	SVM, NB [55]	Leave 01 Trial Out	No Segmentation	60.1	63.5
	CNN (Current Study)	80% - 20%	12s (6s)	**90.75**	**91.01**
NMI	SVM [51]	80% - 20%	No Segmentation	75.16	74.41
	CNN (Current Study)	80% - 20%	8s (4s) for Valence, 12s (6s) for Arousal	**91.26**	**91.23**
TE	DARCNN [23]	10 Fold CV	3s (2.5s)	**89.06**	**89.73**
		Leave 01 Subject Out	3s (2.5s)	81.50	81.39
	CNN (Current Study)	80% - 20%	12 (6s)	73.80	74.36

Among the functional connectivity methods, non-linear methods (e.g., MI) provide higher ER accuracies than linear methods (e.g., PCC). The nervous system of Homo sapiens is very complex. Complex nonlinear phenomena happen from the neuron cell to the entire nervous system. However, linear connectivity analysis methods like correlation and coherence have been widely used over decades for their simplicity in measuring neural connectivity and interconnections. But, modern studies reported that these linear methods could only deal with limited neural activities and their functional relationships, and therefore, they cannot accurately identify neural behaviors. Therefore, nonlinear methods are essential to investigate neuronal processing and signal transfer more accurately and realistically [76]. Nonlinear approaches can promisingly provide deep insights into neurophysiological mechanisms. Hence the nonlinear techniques have the potential to develop improved EEG-based ER systems.

B. ER PERFORMANCE IN DIFFERENT BANDS

In this study, we have designed a CNN classifier for emotion classification. Six different connectivity features have been inspected in three different frequency bands. The best accuracy is obtained in the Gamma band (91.26% for valence and 91.23% for Arousal with the NMI feature).

The cognitive, vigilance or emotional activities of brain can be prominent in some specific frequency bands. Therefore, EEG signals from the standard Alpha, Beta, and Gamma bands have been used in this study to search for the most suitable frequency band for ER and to investigate the performance of connectivity methods in different bands. The experiential results suggest that the high-frequency bands, especially the Gamma band, are sensitive to emotion alteration for each connectivity method. A significant part of the literature agrees with these findings that the brain's emotional actions are associated with the Gamma band, which keeps more trustworthy and prominent properties [36], [77], [78]. Zhuang et al. [79] used the empirical mode decomposition to recognize the emotion types. Their results indicated that the performance of Beta and Gamma bands are more influential than other bands. Liu et al. [80] and Chen et al. [46] performed ER using connectivity features extracted from the different frequency bands of the EEG signals and suggested that the high-frequency bands were more suitable for ER. The authors of the study [46] found that connectivity features extracted from signals from high-frequency bands are more informative than signals from low-frequency bands. The study [81] also used the DEAP dataset to classify emotion from EEG signals from five sub-frequency bands and the full-frequency band and showed that recognition accuracy in the Gamma band was higher than in the full-frequency band and other lower-frequency bands.

Emotion might create intense memories which can last long. The emotion-stimulated memory initiates the activation

of diffusely projecting neuro-modulatory systems, which in turn increase the consolidation of synaptic plasticity in the activated regions. This process needs the propagation of signals between brain regions to induce long-lasting synaptic plasticity. These requirements are satisfied by the Gamma oscillations of EEG, which is a synchronous activity on a fast timescale (35–120 Hz) [82]. Thus, the higher emotion recognition accuracy in the Gamma frequency band is justified.

VI. CONCLUSION

This paper has presented a thorough investigation of prominent connectivity features for human emotion recognition from EEG to indicate how distinct brain connectivity is well-informative as features for emotion classification. For this accomplishment, brain area connectivity is assessed for classifying emotions by using 32 channels of EEG signals. After segmenting and filtering the data in the preprocessing stage, features are extracted by applying six connectivity techniques, including XCOR, PCC, PLV, MI, NMI, and TE, which have been selected through an extensive review. Each type of feature is represented in a 2D map individually. Finally, a customized CNN model is used to classify the feature maps, followed by a rigorous classification accuracy analysis. MI-based connectivity (i.e., MI and NMI) have been identified as the more accurate methods in the Gamma frequency band, with accuracy percentages of 90.75% and 91.26% for valence and 91.01% and 91.23% for arousal, respectively. It is clearly seen that the connectivity features extracted from the higher-frequency band achieved a more accurate results than the features extracted from the lower-frequency band. The findings of this study are anticipated to be helpful for the research and development of efficient emotion recognition system.

Existing researches proposed a variety of approaches to measure and analyze brain network connectivity. Although six connectivity measurement methods are applied (XCOR, PCC, PLV, MI, NMI, and TE) and compared their effectiveness, consideration of more methods could enhance the support to prominent feature findings of this study. The first-order TE feature is used in this study without considering the time delay. The performance of the TE feature can be improved further if there is more freedom of parameter selection. Moreover, a CNN model is used as a classifier. Other types of classifiers may alter the results with better accuracy. Here, only the inter-channel connectivity is considered. On the other hand, the intra-channel connectivity might also be a viable alternative for future work. Other connectivity methods can also be used to explore the best connectivity method.

REFERENCES

[1] M. R. Islam, M. A. Moni, M. M. Islam, M. Rashed-Al-Mahfuz, M. S. Islam, M. K. Hasan, M. S. Hossain, M. Ahmad, S. Uddin, A. Azad, S. A. Alyami, M. A. R. Ahad, and P. Lio, "Emotion recognition from EEG signal focusing on deep learning and shallow learning techniques," *IEEE Access*, vol. 9, pp. 94601–94624, 2021, doi: 10.1109/ACCESS.2021.3091487.

[2] A. Khattak, M. Z. Asghar, M. Ali, and U. Batool, "An efficient deep learning technique for facial emotion recognition," *Multimedia Tools Appl.*, vol. 81, no. 2, pp. 1649–1683, Jan. 2022, doi: 10.1007/s11042-021-11298-w.

[3] E. Morais, R. Hoory, W. Zhu, I. Gat, M. Damasceno, and H. Aronowitz, "Speech emotion recognition using self-supervised features," in *Proc. IEEE Int. Conf. Acoust., Speech Signal Process. (ICASSP)*, May 2022, pp. 6922–6926, doi: 10.1109/ICASSP43922.2022.9747870.

[4] L. Kessous, G. Castellano, and G. Caridakis, "Multimodal emotion recognition in speech-based interaction using facial expression, body gesture and acoustic analysis," *J. Multimodal User Interfaces*, vol. 3, nos. 1–2, pp. 33–48, Mar. 2010, doi: 10.1007/s12193-009-0025-5.

[5] Y. Gao, X. Wang, T. Potter, J. Zhang, and Y. Zhang, "Single-trial EEG emotion recognition using Granger causality/transfer entropy analysis," *J. Neurosci. Methods*, vol. 346, Dec. 2020, Art. no. 108904, doi: 10.1016/j.jneumeth.2020.108904.

[6] S. M. Alarcão and M. J. Fonseca, "Emotions recognition using EEG signals: A survey," *IEEE Trans. Affective Comput.*, vol. 10, no. 3, pp. 374–393, Jul./Sep. 2019, doi: 10.1109/TAFFC.2017.2714671.

[7] S.-E. Moon, C.-J. Chen, C.-J. Hsieh, J.-L. Wang, and J.-S. Lee, "Emotional EEG classification using connectivity features and convolutional neural networks," *Neural Netw.*, vol. 132, pp. 96–107, Dec. 2020, doi: 10.1016/j.neunet.2020.08.009.

[8] M. R. Islam, M. M. Islam, M. M. Rahman, C. Mondal, S. K. Singha, M. Ahmad, A. Awal, M. S. Islam, and M. A. Moni, "EEG channel correlation based model for emotion recognition," *Comput. Biol. Med.*, vol. 136, Sep. 2021, Art. no. 104757, doi: 10.1016/j.compbiomed.2021.104757.

[9] S. Paradiso, N. C. Andreasen, B. Crespo-Facorro, D. S. O'Leary, G. L. Watkins, L. L. Boles Ponto, and R. D. Hichwa, "Emotions in unmedicated patients with schizophrenia during evaluation with positron emission tomography," *Amer. J. Psychiatry*, vol. 160, no. 10, pp. 1775–1783, Oct. 2003, doi: 10.1176/appi.ajp.160.10.1775.

[10] S. Koelsch, T. Fritz, K. Müller, A. D. Friederici, and D. Y. Cramon, "Investigating emotion with music: An fMRI study," *Human Brain Mapping*, vol. 27, no. 3, pp. 239–250, Mar. 2006, doi: https://doi.org/10.1002/hbm.20180.

[11] H. Adeli and S. Ghosh-Dastidar, "Wavelet-chaos methodology for analysis of EEGs and EEG sub-bands," in *Automated EEG-Based Diagnosis of Neurological Disorders*, vol. 54, no. 2. Boca Raton, FL, USA: CRC Press, 2010, pp. 119–141, doi: 10.1201/9781439815328-c7.

[12] E. L. van den Broek, "Ubiquitous emotion-aware computing," *Pers. Ubiquitous Comput.*, vol. 17, no. 1, pp. 53–67, Jan. 2013, doi: 10.1007/s00779-011-0479-9.

[13] J. A. Russell, "A circumplex model of affect," *J. Personality Social Psychol.*, vol. 39, no. 6, pp. 1161–1178, Dec. 1980, doi: https://doi.org/10.1037/h0077714.

[14] A. Mehrabian, "Comparison of the PAD and PANAS as models for describing emotions and for differentiating anxiety from depression," *J. Psychopathology Behav. Assessment*, vol. 19, no. 4, pp. 331–357, Dec. 1997, doi: 10.1007/BF02229025.

[15] L. Shu, J. Xie, M. Yang, Z. Li, Z. Li, D. Liao, X. Xu, and X. Yang, "A review of emotion recognition using physiological signals," *Sensors*, vol. 18, no. 7, p. 2074, Jun. 2018, doi: 10.3390/s18072074.

[16] J. Liu, G. Wu, Y. Luo, S. Qiu, S. Yang, W. Li, and Y. Bi, "EEG-based emotion classification using a deep neural network and sparse autoencoder," *Frontiers Syst. Neurosci.*, vol. 14, p. 43, Sep. 2020, doi: 10.3389/fnsys.2020.00043.

[17] J. Li, Z. Zhang, and H. He, "Hierarchical convolutional neural networks for EEG-based emotion recognition," *Cogn. Comput.*, vol. 10, no. 2, pp. 368–380, 2018, doi: 10.1007/s12559-017-9533-x.

[18] S. Liu, J. Tong, J. Meng, J. Yang, X. Zhao, F. He, H. Qi, and D. Ming, "Study on an effective cross-stimulus emotion recognition model using EEGs based on feature selection and support vector machine," *Int. J. Mach. Learn. Cybern.*, vol. 9, no. 5, pp. 721–726, May 2018, doi: 10.1007/s13042-016-0601-4.

[19] K. J. Friston, "Functional and effective connectivity: A review," *Brain Connectivity*, vol. 1, no. 1, pp. 13–36, Jan. 2011, doi: 10.1089/brain.2011.0008.

[20] G. Niso, R. Bruña, E. Pereda, R. Gutiérrez, R. Bajo, F. Maestú, and F. del-Pozo, "HERMES: Towards an integrated toolbox to characterize functional and effective brain connectivity," *Neuroinformatics*, vol. 11, no. 4, pp. 405–434, Oct. 2013, doi: 10.1007/s12021-013-9186-1.

[21] S.-E. Moon, S. Jang, and J.-S. Lee, "Convolutional neural network approach for EEG-based emotion recognition using brain connectivity and its spatial information," in *Proc. IEEE Int. Conf. Acoust., Speech Signal Process. (ICASSP)*, Apr. 2018, pp. 2556–2560, doi: 10.1109/ICASSP.2018.8461315.

[22] T. F. Tafreshi, M. R. Daliri, and M. Ghodousi, "Functional and effective connectivity based features of EEG signals for object recognition," *Cognit. Neurodynamics*, vol. 13, no. 6, pp. 555–566, Dec. 2019, doi: 10.1007/s11571-019-09556-7.

[23] J. Chen, C. Min, C. Wang, Z. Tang, Y. Liu, and X. Hu, "Electroencephalograph-based emotion recognition using brain connectivity feature and domain adaptive residual convolution model," *Frontiers Neurosci.*, vol. 16, Jun. 2022, Art. no. 878146, doi: 10.3389/fnins.2022.878146.

[24] S. Farashi and R. Khosrowabadi, "EEG based emotion recognition using minimum spanning tree," *Phys. Eng. Sci. Med.*, vol. 43, no. 3, pp. 985–996, Sep. 2020, doi: 10.1007/s13246-020-00895-y.

[25] R. Zhang, Z. Wang, and Y. Liu, "The research of EEG feature extraction and classification for subjects with different organizational commitment," in *Proc. MATEC Web Conf.*, vol. 355, 2022, p. 03042, doi: 10.1051/matecconf/202235503042.

[26] A. Mert and A. Akan, "Emotion recognition based on time–frequency distribution of EEG signals using multivariate synchrosqueezing transform," *Digit. Signal Process.*, vol. 81, pp. 106–115, Oct. 2018, doi: 10.1016/j.dsp.2018.07.003.

[27] H. Yang, S. Huang, S. Guo, and G. Sun, "Multi-classifier fusion based on MI–SFFS for cross-subject emotion recognition," *Entropy*, vol. 24, no. 5, p. 705, May 2022, doi: 10.3390/e24050705.

[28] R. M. Mehmood, M. Bilal, S. Vimal, and S.-W. Lee, "EEG-based affective state recognition from human brain signals by using hjorth-activity," *Measurement*, vol. 202, Oct. 2022, Art. no. 111738, doi: 10.1016/j.measurement.2022.111738.

[29] E. S. Pane, A. D. Wibawa, and M. H. Purnomo, "Improving the accuracy of EEG emotion recognition by combining valence lateralization and ensemble learning with tuning parameters," *Cognit. Process.*, vol. 20, no. 4, pp. 405–417, Nov. 2019, doi: 10.1007/s10339-019-00924-z.

[30] Z. Yin, L. Liu, J. Chen, B. Zhao, and Y. Wang, "Locally robust EEG feature selection for individual-independent emotion recognition," *Exp. Syst. Appl.*, vol. 162, Dec. 2020, Art. no. 113768, doi: 10.1016/j.eswa.2020.113768.

[31] A. Subasi, T. Tuncer, S. Dogan, D. Tanko, and U. Sakoglu, "EEG-based emotion recognition using tunable Q wavelet transform and rotation forest ensemble classifier," *Biomed. Signal Process. Control*, vol. 68, Jul. 2021, Art. no. 102648, doi: 10.1016/j.bspc.2021.102648.

[32] L. A. Moctezuma, T. Abe, and M. Molinas, "Two-dimensional CNN-based distinction of human emotions from EEG channels selected by multi-objective evolutionary algorithm," *Sci. Rep.*, vol. 12, no. 1, p. 3523, Mar. 2022, doi: 10.1038/s41598-022-07517-5.

[33] Y. Li, J. Huang, H. Zhou, and N. Zhong, "Human emotion recognition with electroencephalographic multidimensional features by hybrid deep neural networks," *Appl. Sci.*, vol. 7, no. 10, p. 1060, Oct. 2017, doi: 10.3390/app7101060.

[34] A. Topic and M. Russo, "Emotion recognition based on EEG feature maps through deep learning network," *Eng. Sci. Technol., Int. J.*, vol. 24, no. 6, pp. 1442–1454, Dec. 2021, doi: 10.1016/j.jestch.2021.03.012.

[35] T. Song, W. Zheng, P. Song, and Z. Cui, "EEG emotion recognition using dynamical graph convolutional neural networks," *IEEE Trans. Affect. Comput.*, vol. 11, no. 3, pp. 532–541, Jul./Sep. 2020, doi: 10.1109/TAFFC.2018.2817622.

[36] C. Wei, L.-L. Chen, Z.-Z. Song, X.-G. Lou, and D.-D. Li, "EEG-based emotion recognition using simple recurrent units network and ensemble learning," *Biomed. Signal Process. Control*, vol. 58, Apr. 2020, Art. no. 101756, doi: 10.1016/j.bspc.2019.101756.

[37] L. Liu, Y. Ji, Y. Gao, T. Li, and W. Xu, "A data-driven adaptive emotion recognition model for college students using an improved multifeature deep neural network technology," *Comput. Intell. Neurosci.*, vol. 2022, pp. 1–9, May 2022, doi: 10.1155/2022/1343358.

[38] R. Khosrowabadi, M. Heijnen, A. Wahab, and H. C. Quek, "The dynamic emotion recognition system based on functional connectivity of brain regions," in *Proc. IEEE Intell. Vehicles Symp.*, Jun. 2010, pp. 377–381, doi: 10.1109/IVS.2010.5548102.

[39] P. C. Petrantonakis and L. J. Hadjileontiadis, "A novel emotion elicitation index using frontal brain asymmetry for enhanced EEG-based emotion recognition," *IEEE Trans. Inf. Technol. Biomed.*, vol. 15, no. 5, pp. 737–746, Sep. 2011, doi: 10.1109/TITB.2011.2157933.

[40] J. Z. Y. Gao, Z. Cao, and J. Liu, "A novel dynamic brain network in arousal for brain states and emotion analysis," *Math. Biosciences Eng.*, vol. 18, no. 6, pp. 7440–7463, 2021, doi: 10.3934/mbe.2021368.

[41] J. S. Ramakrishna, N. Sinha, and H. Ramasangu, "Classification of human emotions using EEG-based causal connectivity patterns," in *Proc. IEEE Conf. Comput. Intell. Bioinf. Comput. Biol. (CIBCB)*, Oct. 2021, pp. 1–8, doi: 10.1109/CIBCB49929.2021.9562837.

[42] W. Wang, "Brain network features based on theta-gamma cross-frequency coupling connections in EEG for emotion recognition," *Neurosci. Lett.*, vol. 761, Sep. 2021, Art. no. 136106, doi: 10.1016/j.neulet.2021.136106.

[43] D. S. Naser and G. Saha, "Influence of music liking on EEG based emotion recognition," *Biomed. Signal Process. Control*, vol. 64, Feb. 2021, Art. no. 102251, doi: 10.1016/j.bspc.2020.102251.

[44] B. Kılıç and S. Aydın, "Classification of contrasting discrete emotional states indicated by EEG based graph theoretical network measures," *Neuroinformatics*, vol. 20, no. 4, pp. 863–877, Oct. 2022, doi: 10.1007/s12021-022-09579-2.

[45] M. Zanetti, L. Faes, M. D. Cecco, A. Fornaser, M. Valente, G. Guandalini, and G. Nollo, "Assessment of mental stress through the analysis of physiological signals acquired from wearable devices," in *Italian Forum of Ambient Assisted Living*, vol. 544, A. Leone, A. Caroppo, G. Rescio, G. Diraco, and P. Siciliano, Eds. Cham, Switzerland: Springer, 2019, pp. 243–256, doi: 10.1007/978-3-030-05921-7_20.

[46] M. Chen, J. Han, L. Guo, J. Wang, and I. Patras, "Identifying valence and arousal levels via connectivity between EEG channels," in *Proc. Int. Conf. Affect. Comput. Intell. Interact. (ACII)*, Sep. 2015, pp. 63–69, doi: 10.1109/ACII.2015.7344552.

[47] M. Yu, S. Xiao, M. Hua, H. Wang, X. Chen, F. Tian, and Y. Li, "EEG-based emotion recognition in an immersive virtual reality environment: From local activity to brain network features," *Biomed. Signal Process. Control*, vol. 72, Feb. 2022, Art. no. 103349, doi: 10.1016/j.bspc.2021.103349.

[48] P. Sarma and S. Barma, "Emotion recognition by discriminating EEG segments with high affective content from automatically selected relevant channels," *IEEE Trans. Instrum. Meas.*, vol. 71, pp. 1–12, 2022, doi: 10.1109/TIM.2022.3147876.

[49] Q. Kang, Q. Gao, Y. Song, Z. Tian, Y. Yang, Z. Mao, and E. Dong, "Emotion recognition from EEG signals of hearing-impaired people using stacking ensemble learning framework based on a novel brain network," *IEEE Sensors J.*, vol. 21, no. 20, pp. 23245–23255, Oct. 2021, doi: 10.1109/JSEN.2021.3108471.

[50] R. Khosrowabadi, "Stress and perception of emotional stimuli: long-term stress rewiring the brain," *Basic Clin. Neurosci. J.*, vol. 9, no. 2, pp. 107–120, Mar. 2018, doi: 10.29252/NIRP.BCN.9.2.107.

[51] Z. Wang, S. Hu, and H. Song, "Channel selection method for EEG emotion recognition using normalized mutual information," *IEEE Access*, vol. 7, pp. 143303–143311, 2019, doi: 10.1109/ACCESS.2019.2944273.

[52] P. Li, H. Liu, Y. Si, C. Li, F. Li, X. Zhu, X. Huang, Y. Zeng, D. Yao, Y. Zhang, and P. Xu, "EEG based emotion recognition by combining functional connectivity network and local activations," *IEEE Trans. Biomed. Eng.*, vol. 66, no. 10, pp. 2869–2881, Oct. 2019, doi: 10.1109/TBME.2019.2897651.

[53] J. Pan, F. Yang, L. Qiu, and H. Huang, "Fusion of EEG-based activation, spatial, and connection patterns for fear emotion recognition," *Comput. Intell. Neurosci.*, vol. 2022, Apr. 2022, Art. no. 3854513, doi: 10.1155/2022/3854513.

[54] C. Chen, Z. Li, F. Wan, L. Xu, A. Bezerianos, and H. Wang, "Fusing frequency-domain features and brain connectivity features for cross-subject emotion recognition," *IEEE Trans. Instrum. Meas.*, vol. 71, pp. 1–15, 2022, doi: 10.1109/TIM.2022.3168927.

[55] P. Arnau-González, M. Arevalillo-Herráez, and N. Ramzan, "Fusing highly dimensional energy and connectivity features to identify affective states from EEG signals," *Neurocomputing*, vol. 244, pp. 81–89, Jun. 2017, doi: 10.1016/j.neucom.2017.03.027.

[56] Y. Kumagai, M. Arvaneh, H. Okawa, T. Wada, and T. Tanaka, "Classification of familiarity based on cross-correlation features between EEG and music," in *Proc. 39th Annu. Int. Conf. IEEE Eng. Med. Biol. Soc. (EMBC)*, Jul. 2017, pp. 2879–2882, doi: 10.1109/EMBC.2017.8037458.

[57] K. Guo, H. Mei, X. Xie, and X. Xu, "A convolutional neural network feature fusion framework with ensemble learning for EEG-based emotion classification," in *Proc. IEEE MTT-S Int. Microw. Biomed. Conf. (IMBioC)*, May 2019, pp. 1–4, doi: 10.1109/IMBIOC.2019.8777738.

[58] H. Wang, K. Liu, F. Qi, X. Deng, and P. Li, "EEG-based emotion recognition using convolutional neural network with functional connections," in *Cognitive Systems and Signal Processing*. Singapore: Springer, 2021, pp. 33–40, doi: 10.1007/978-981-16-2336-3_3.

[59] H. Liu, J. Zhang, Q. Liu, and J. Cao, "Minimum spanning tree based graph neural network for emotion classification using EEG," *Neural Netw.*, vol. 145, pp. 308–318, Jan. 2022, doi: 10.1016/j.neunet.2021.10.023.

[60] G. Bao, K. Yang, L. Tong, J. Shu, R. Zhang, L. Wang, B. Yan, and Y. Zeng, "Linking multi-layer dynamical GCN with style-based recalibration CNN for EEG-based emotion recognition," *Frontiers Neurorobotics*, vol. 16, Feb. 2022, Art. no. 834952, doi: 10.3389/fnbot.2022.834952.

[61] Z. Wang, Y. Liu, R. Zhang, J. Zhang, and X. Guo, "EEG-based emotion recognition using partial directed coherence dense graph propagation," in *Proc. 14th Int. Conf. Measuring Technol. Mechatronics Autom. (ICMTMA)*, Jan. 2022, pp. 610–617, doi: 10.1109/ICMTMA54903.2022.00127.

[62] F. Zheng, B. Hu, X. Zheng, C. Ji, J. Bian, and X. Yu, "Dynamic differential entropy and brain connectivity features based EEG emotion recognition," *Int. J. Intell. Syst.*, vol. 37, no. 12, pp. 12511–12533, Dec. 2022, doi: 10.1002/int.23096.

[63] L. Jin and E. Y. Kim, "Interpretable cross-subject EEG-based emotion recognition using channel-wise features," *Sensors*, vol. 20, no. 23, p. 6719, Nov. 2020, doi: 10.3390/s20236719.

[64] S. Bagherzadeh, K. Maghooli, A. Shalbaf, and A. Maghsoudi, "Recognition of emotional states using frequency effective connectivity maps through transfer learning approach from electroencephalogram signals," *Biomed. Signal Process. Control*, vol. 75, May 2022, Art. no. 103544, doi: 10.1016/j.bspc.2022.103544.

[65] S. Bagherzadeh, K. Maghooli, A. Shalbaf, and A. Maghsoudi, "Emotion recognition using effective connectivity and pre-trained convolutional neural networks in EEG signals," *Cogn. Neurodyn.*, vol. 6, pp. 1087–1106, Jan. 2022 doi: 10.1007/s11571-021-09756-0.

[66] H. Chao, L. Dong, Y. Liu, and B. Lu, "Improved deep feature learning by synchronization measurements for multi-channel EEG emotion recognition," *Complexity*, vol. 2020, pp. 1–15, Mar. 2020, doi: 10.1155/2020/6816502.

[67] Y. Tang, D. Chen, H. Liu, C. Cai, and X. Li, "Deep EEG superresolution via correlating brain structural and functional connectivities," *IEEE Trans. Cybern.*, early access, Jun. 14, 2022, doi: 10.1109/TCYB.2022.3178370.

[68] Z. Li, G. Zhang, L. Wang, J. Wei, and J. Dang, "Emotion recognition using spatial–temporal EEG features through convolutional graph attention network," *J. Neural Eng.*, vol. 20, no. 1, Feb. 2023, Art. no. 016046, doi: 10.1088/1741-2552/acb79e.

[69] S. Koelstra, C. Muhl, M. Soleymani, J.-S. Lee, A. Yazdani, T. Ebrahimi, T. Pun, A. Nijholt, and I. Patras, "DEAP: A database for emotion analysis ;using physiological signals," *IEEE Trans. Affect. Comput.*, vol. 3, no. 1, pp. 18–31, Jan. 2012, doi: 10.1109/T-AFFC.2011.15.

[70] T. Alotaiby, F. E. A. El-Samie, S. A. Alshebeili, and I. Ahmad, "A review of channel selection algorithms for EEG signal processing," *EURASIP J. Adv. Signal Process.*, vol. 2015, no. 1, Dec. 2015, doi: 10.1186/s13634-015-0251-9.

[71] A. Delorme and S. Makeig, "EEGLAB: An open source toolbox for analysis of single-trial EEG dynamics including independent component analysis," *J. Neurosci. Methods*, vol. 134, no. 1, pp. 9–21, Mar. 2004, doi: 10.1016/j.jneumeth.2003.10.009.

[72] P. N. Paranjape, M. M. Dhabu, P. S. Deshpande, and A. M. Kekre, "Cross-correlation aided ensemble of classifiers for BCI oriented EEG study," *IEEE Access*, vol. 7, pp. 11985–11996, 2019, doi: 10.1109/ACCESS.2019.2892492.

[73] J. T. Oliva and J. L. Garcia Rosa, "How an epileptic EEG segment, used as reference, can influence a cross-correlation classifier?" *Int. J. Speech Technol.*, vol. 47, no. 1, pp. 178–196, Jul. 2017, doi: 10.1007/s10489-016-0891-y.

[74] C. E. Shannon, "A mathematical theory of communication," *Bell Syst. Tech. J.*, vol. 27, no. 3, pp. 379–423, 1948, doi: 10.1002/j.1538-7305.1948.tb01338.x.

[75] M. A. H. Akhand, *Deep Learning Fundamentals—A Practical Approach to Understanding Deep Learning Methods*. Dhaka, Bangladesh: Univ. Grants Commission Bangladesh, 2021.

[76] F. He and Y. Yang, "Nonlinear system identification of neural systems from neurophysiological signals," *Neuroscience*, vol. 458, pp. 213–228, Mar. 2021, doi: 10.1016/j.neuroscience.2020.12.001.

[77] A. E. Vijayan, D. Sen, and A. P. Sudheer, "EEG-based emotion recognition using statistical measures and auto-regressive modeling," in *Proc. IEEE Int. Conf. Comput. Intell. Commun. Technol. (CICT)*, Apr. 2015, pp. 587–591, doi: 10.1109/CICT.2015.24.

[78] Z. Mohammadi, J. Frounchi, and M. Amiri, "Wavelet-based emotion recognition system using EEG signal," *Neural Comput. Appl.*, vol. 28, no. 8, pp. 1985–1990, Aug. 2017, doi: 10.1007/s00521-015-2149-8.

[79] N. Zhuang, Y. Zeng, L. Tong, C. Zhang, H. Zhang, and B. Yan, "Emotion recognition from EEG signals using multidimensional information in EMD domain," *BioMed Res. Int.*, vol. 2017, pp. 1–9, Aug. 2017, doi: 10.1155/2017/8317357.

[80] X. Liu, T. Li, C. Tang, T. Xu, P. Chen, A. Bezerianos, and H. Wang, "Emotion recognition and dynamic functional connectivity analysis based on EEG," *IEEE Access*, vol. 7, pp. 143293–143302, 2019, doi: 10.1109/ACCESS.2019.2945059.

[81] J. Bi, F. Wang, X. Yan, J. Ping, and Y. Wen, "Multi-domain fusion deep graph convolution neural network for EEG emotion recognition," *Neural Comput. Appl.*, vol. 34, no. 24, pp. 22241–22255, Dec. 2022, doi: 10.1007/s00521-022-07643-1.

[82] D. B. Headley and D. Paré, "In sync: Gamma oscillations and emotional memory," *Frontiers Behav. Neurosci.*, vol. 7, p. 170, Nov. 2013, doi: 10.3389/fnbeh.2013.00170.

MAHFUZA AKTER MARIA received the B.Sc. degree in computer science and engineering from Patuakhali Science and Technology University, Bangladesh, in 2019, and the M.Sc. degree in computer science and engineering from the Khulna University of Engineering and Technology, Bangladesh, in 2022.

Her research interests include affective computing, pattern recognition, and machine learning.

M. A. H. AKHAND (Senior Member, IEEE) received the B.Sc. degree in electrical and electronic engineering from the Khulna University of Engineering and Technology (KUET), Bangladesh, in 1999, and the M.E. degree in human and artificial intelligent systems and the Ph.D. degree in system design engineering from the University of Fukui, Japan, in 2006 and 2009, respectively.

He joined as a Lecturer with the Department of Computer Science and Engineering, KUET, in 2001, where he has been a Professor, since 2014. He is currently the Head of the Computational Intelligence Research Group, Department of Computer Science and Engineering, KUET. He has more than 150 research publications. His research interests include artificial neural networks, evolutionary computation, bioinformatics, swarm intelligence, and other bio-inspired computing techniques.

Dr. Akhand is a Life Member of the Institution of Engineers, Bangladesh (IEB) and a Life Time Member of the Bangladesh Computer Society (BCS). He received several best paper prizes in international conferences.

A. B. M. AOWLAD HOSSAIN (Senior Member, IEEE) received the B.Sc. degree in electrical and electronic engineering from the Khulna University of Engineering and Technology (KUET), Bangladesh, in 2002, the M.Sc. degree in electrical and electronic engineering from the Bangladesh University of Engineering Technology (BUET), Bangladesh, in 2005, and the Doctor of Philosophy degree in biomedical engineering from Kyung Hee University, South Korea, in 2012.

He has been a Professor with the Department of Electronics and Communication Engineering, KUET, since 2015. He has published more than 60 research articles. His research interests include computer aided diagnosis, machine learning, medical imaging systems, and the modeling and simulation of physiological systems.

Dr. Hossain is a Life Fellow of the Institution of Engineers, Bangladesh. He has received awards for best papers in two IEEE co-sponsored international conferences.

MD. ABDUS SAMAD KAMAL (Senior Member, IEEE) received the B.Sc.Eng. degree from the Khulna University of Engineering and Technology (KUET), Bangladesh, in 1997, and the master's and Ph.D. degrees from Kyushu University, Japan, in 2003 and 2006, respectively.

He was a Lecturer with KUET, from 1997 to 2000; a Researcher with Kyushu University, in 2006 and from 2008 to 2011; an Assistant Professor with International Islamic University Malaysia, Malaysia, from 2006 to 2008; and a Researcher with The University of Tokyo, Japan, from 2011 to 2014. He worked as a Visiting Researcher with Toyota Central R&D Labs., Inc., Japan, from 2014 to 2016. He was a Senior Lecturer with the School of Engineering, Monash University Malaysia, from 2016 to 2019. Currently, he is an Associate Professor with the Graduate School of Science and Technology, Gunma University, Japan. His research interests include intelligent transportation systems, connected and automated vehicles, and the applications of machine learning and model predictive control.

Dr. Kamal is a member of the Society of Instrument and Control Engineers (SICE) and a Chartered Engineer of the Institution of Engineering and Technology (IET).

KOU YAMADA (Member, IEEE) was born in Akita, Japan, in 1964. He received the B.S. and M.S. degrees from Yamagata University, Yamagata, Japan, in 1987 and 1989, respectively, and the Dr.Eng. degree from Osaka University, Osaka, Japan, in 1997.

From 1991 to 2000, he was with the Department of Electrical and Information Engineering, Yamagata University, as a Research Associate. From 2000 to 2008, he was an Associate Professor with the Department of Mechanical System Engineering, Gunma University, Gunma, Japan, where he has been a Professor, since 2008. His research interests include robust control, repetitive control, process control and control theory for inverse systems, and infinite-dimensional systems.

Dr. Yamada is a member of SICE. He received the 2005 Yokoyama Award in Science and Technology, the 2005 Electrical Engineering/Electronics, Computer, Telecommunication and Information Technology International Conference (ECTI-CON2005) Best Paper Award, the Japanese Ergonomics Society Encouragement Award for Academic Paper, in 2007, the 2008 Electrical Engineering/Electronics, Computer, Telecommunication and Information Technology International Conference (ECTI-CON2008) Best Paper Award, the Fourth International Conference on Innovative Computing, Information and Control Best Paper Award, in 2009, the 14th International Conference on Innovative Computing, Information and Control Best Paper Award, in 2019, and the Outstanding Achievement Award from the Kanto Branch of Japanese Society for Engineering Education, in 2022.